Overexpression of enhancer of zeste homolog 2 with trimethylation of lysine 27 on histone H3 in adult T-cell leukemia/lymphoma as a target for epigenetic therapy

Daisuke Sasaki,[1] Yoshitaka Imaizumi,[2] Hiroo Hasegawa,[1] Akemi Osaka,[1] Kunihiro Tsukasaki,[2] Young Lim Choi,[3] Hiroyuki Mano,[3] Victor E. Marquez,[4] Tomayoshi Hayashi,[5] Katsunori Yanagihara,[1] Yuji Moriwaki,[2] Yasushi Miyazaki,[2] Shimeru Kamihira,[1] and Yasuaki Yamada[1]

[1]Department of Laboratory Medicine, Nagasaki University Graduate School of Biomedical Sciences, Nagasaki, Japan; [2]Department of Hematology and Molecular Medicine, Atomic Bomb Disease Institute, Nagasaki University Graduate School of Biomedical Sciences, Nagasaki, Japan; [3]Division of Functional Genomics, Jichi Medical University, Tochigi, Japan; [4]Chemical Biology Laboratory, National Cancer Institute, Frederick, MD, USA; and [5]Department of Pathology, Nagasaki University Hospital, Nagasaki, Japan

ABSTRACT

Background
Enhancer of zeste homolog 2 is a component of the Polycomb repressive complex 2 that mediates chromatin-based gene silencing through trimethylation of lysine 27 on histone H3. This complex plays vital roles in the regulation of development-specific gene expression.

Design and Methods
In this study, a comparative microarray analysis of gene expression in primary adult T-cell leukemia/lymphoma samples was performed, and the results were evaluated for their oncogenic and clinical significance.

Results
Significantly higher levels of Enhancr of zeste homolog 2 and RING1 and YY1 binding protein transcripts with enhanced levels of trimethylation of lysine 27 on histone H3 were found in adult T-cell leukemia/lymphoma cells compared with those in normal CD4+ T cells. Furthermore, there was an inverse correlation between the expression level of Enhancer of zeste homolog 2 and that of miR-101 or miR-128a, suggesting that the altered expression of the latter miRNAs accounts for the overexpression of the former. Patients with high Enhancer of zeste homolog 2 or RING1 and YY1 binding protein transcripts had a significantly worse prognosis than those without it, indicating a possible role of these genes in the oncogenesis and progression of this disease. Indeed, adult T-cell leukemia/lymphoma cells were sensitive to a histone methylation inhibitor, 3-deazaneplanocin A. Furthermore, 3-deazaneplanocin A and histone deacetylase inhibitor panobinostat showed a synergistic effect in killing the cells

Conclusions
These findings reveal that adult T-cell leukemia/lymphoma cells have deregulated Polycomb repressive complex 2 with over-expressed Enhancer of zeste homolog 2, and that there is the possibility of a new therapeutic strategy targeting histone methylation in this disease.

Key words: adult T-cell leukemia/lymphoma, human T-cell leukemia virus type-1, Enhancer of zeste homolog 2, H3K27me3.

Citation: Sasaki D, Imaizumi Y, Hasegawa H, Osaka A, Tsukasaki K, Choi YL, Mano H, Marquez VE, Hayashi T, Yanagihara K, Moriwaki Y, Miyazaki Y, Kamihira S, and Yamada Y. Overexpression of enhancer of zeste homolog 2 with trimethylation of lysine 27 on histone H3 in adult T-cell leukemia/lymphoma as a target for epigenetic therapy Haematologica 2011;96(4):712-719. doi:10.3324/haematol.2010.028605

Funding: supported in part by a Grant-in-Aid for Scientific Research from the Ministry of Health, Labour, and Welfare of Japan (N. 04010119). For VEM, this research was supported in part by the Intramural Research Program of the NIH, Center for Cancer Research, NCI-Frederick.

Acknowledgments: the authors thank Sayaka Mori and Yuko Doi for excellent technical assistance.

Manuscript received June 16, 2010. Revised version arrived on December 16, 2010. Manuscript accepted on December 31, 2010.

Correspondence:
Yasuaki Yamada, Department of Laboratory Medicine, 1-7-1 Sakamoto, Nagasaki 852-8501, Japan. Phone: international +81.958197408.
Fax: international +81.958197422.
E-mail: y-yamada@nagasaki-u.ac.jp

The online version of this article has a Supplementary Appendix.

Introduction

The Polycomb group (PcG) proteins play critical roles in the regulation of development by repressing specific sets of developmental genes through chromatin modification.[1] They form two distinct multimeric complexes, Polycomb repressive complex 1 (PRC1) and PRC2, which bind to polycomb responsive elements (PRE), repress genes required for cell differentiation, and maintain pluripotency and self-renewal of embryonic stem cells and hematopoietic stem cells.[2,3] PRC2 consists of Enhancer of zeste homolog 2 (EZH2), which has histone methyltransferase activity, suppressor of zeste 12 (SUZ12), and embryonic ectoderm development (EED), which is required to maintain the integrity of PRC2.[1,4] Sequence-specific DNA binding protein YY1, which recognizes PRE, interacts with EED and recruits PRC2 to a specific chromatin domain to be repressed.[5] EED interacts with histone deacetylase (HDAC) proteins, HDAC1 and HDAC2, and the histone binding proteins RBBP4 (RbAp48) and RBBP7 (RbAp46).[6] PRC2 thus also participates in histone deacetylation. EZH2, as a part of the PRC2 complex, not only methylates histone but also serves as a recruitment platform for DNA methyltransferases that methylate the promoter regions of target genes, which is another mechanism of gene repression.[7] The more diverse complex PRC1 consists of HPC family proteins that mediate chromatin association, HPH family proteins, RING, BMI1, and others.[1] PRC2 initiates trimethylation of lysine 27 on histone H3 (H3K27me3) and, to a lesser extent, lysine 9 of histone H3.[8] PRC1 recognizes H3K27me3 through the chromodomain of the HPC and maintains the trimethylation. There are a number of reports indicating that such epigenetically mediated transcriptional silencing is associated with cancer development.[1,9] Among these, oncogenic roles of over-expressed EZH2 have been studied in a variety of tumors.[10]

Adult T-cell leukemia/lymphoma (ATL) is a neoplasm of mature CD4+ T-cell origin, etiologically associated with human T-cell leukemia virus type-1 (HTLV-1).[11,12] Its clinical behavior differs among patients and is subclassified into four subtypes: smoldering type and chronic type as indolent subtypes, and acute type and lymphoma type as aggressive subtypes.[13] Inactivation of tumor suppressor genes is one of the key events in development and progression, and there is a strong accumulation of *p14ARF/p15INK4B/p16INK4A* gene deletion/methylation or *p53* gene mutations in aggressive subtypes (>60%).[14-20] In the present study, for further investigation of the oncogenesis of ATL, we performed a comparative microarray analysis of gene expression in primary ATL samples. ATL cells expressed significantly higher levels of *EZH2* and *RYBP* (RING1 and YY1 binding protein) transcripts than CD4+ T cells from healthy volunteers. Moreover, acute-type ATL cells showed significantly higher levels of these transcripts than chronic-type ATL cells, suggesting that deregulation of PcG proteins plays a crucial role not only in the development but also in the progression of ATL. In addition, ATL samples were strongly positive for H3K27me3, and were sensitive to 3-deazaneplanocin A (DZNep), a histone methylation inhibitor.[21-23] It has recently been shown that HDAC inhibitor panobinostat (PS, also known as LBH589) depletes the levels of EZH2, SUZ12, and EED and induces apoptotic death in leukemia cells.[24] Deregulation of PcG protein genes with over-expressed EZH2 in ATL cells suggests that ATL is one of the appropriate target diseases for such epigenetic therapy.

Design and Methods

Sample preparation

This study was approved by the ethics committees of Nagasaki University, and all clinical samples were obtained after written informed consent was provided. The diagnosis of ATL was confirmed by the monoclonal integration of HTLV-1 proviral DNA in the genomic DNA of leukemia cells. Peripheral blood mononuclear cells (PBMCs) were obtained from ATL patients (acute type 22 cases, chronic type 19 cases) and healthy adult volunteers by density gradient centrifugation using Lympho-prep (AXIS SHIELD, Oslo, Norway). For enrichment of ATL cells, CD4 cells were purified from the PBMCs by the magnetic bead method (CD4 MicroBeads, Miltenyi Biotec, Auburn, CA, USA) as described elsewhere.[25] Besides these samples for microarray analysis, we prepared another set of samples for quantitative real-time RT-PCR (qRT-PCR) and Western blotting (25 ATL patients, 13 HTLV-1 carriers, and 12 healthy adults) to confirm the results of microarray analysis. We also used formalin-fixed, paraffin-embedded lymph nodes from 7 patients with lymphoma-type ATL and 5 patients with follicular lymphoma for immunohistochemical analysis.

ATL cell lines used in this study, SO4, ST1, KK1, KOB, and LM-Y1, were established from respective patients in our laboratory and have been confirmed to be of primary ATL cell origin.[26] Cells were maintained in RPMI1640 medium supplemented with 10% FBS and 100 Japan reference units of recombinant interleukin-2 (rIL-2) (kindly provided by Takeda Pharmaceutical Company, Ltd., Osaka, Japan). We also used HTLV-1-infected T-cell lines MT2 and HuT102 and acute T-lymphoblastic leukemia cell lines Jurkat and MOLT4, which were maintained without rIL-2.

DNA microarray analysis

RNA was prepared from purified CD4+ T cells, and subjected to hybridization to HGU133A & B microarray containing 44,760 probe sets for human genes (Affymetrix, Santa Clara, CA, USA) as described previously.[25,27] The mean expression intensity of the internal positive control probe sets (*http://www.affymetrix.com/support/technical/mask_files.affx*) was set to 500 units in each hybridization, and the fluorescence intensity of each test gene was normalized accordingly. All HGU133A & B microarray data are available from the Gene Expression Omnibus website (*http://www.ncbi.nlm.nih.gov/geo*) under the accession number GSE1466.

Quantitative real-time RT-PCR

For confirmation of the results of microarray analysis, we performed quantitative real-time RT-PCR (qRT-PCR) for PcG protein genes. Total RNA was prepared using Isogen (Wako, Osaka, Japan). After removal of contaminated DNA with DNase (Message Clean kit; GenHunter, Nashville, TN, USA), cDNA was constructed from 1 μg of total RNA using the SuperScript III RT-PCR System (Invitrogen, Carlsbad, CA, USA) according to the manufacturer's instructions. Primers and TaqMan probes labeled with TAMRA dye at the 3' end and FAM at the 5' end are listed in *Online Supplementary Table S1*. The mRNA levels for PcG family proteins and porphobilinogen deaminase (PBGD) were measured from a cDNA template using a LightCycler480 PCR System (Roche Diagnostics, Mannheim, Germany). Briefly, reactions were performed in a 20 μL volume with 5 μL (25 ng) of cDNA, 0.5 μM PCR primers, 0.1 μM TaqMan probes, and 10 μL of LightCycler

480 probes Master Mix (Roche Diagnostics). The PCR program consisted of 95°C for 5 min followed by 50 cycles of 95°C for 10 sec and 60°C for 30 sec. After 50 cycles, the absolute amounts of PcG protein mRNA and *PBGD* mRNA were interpolated from the standard curves generated by the dilution method using plasmids derived from a clone transfected with pTAC-1 Vector (BioDynamics Laboratory Inc., Tokyo, Japan) containing amplicons from the PcG family protein and PBGD genes, respectively. To normalize these results for variability in concentration and integrity of RNA and cDNA, the *PBGD* gene was used as an internal control in each sample.

For the quantitative PCR for microRNAs (miRNAs), miR-101, miR-26a, and miR-128a, 10 ng of total RNA (containing miRNA) was used. RT reaction and real-time quantification were performed using TaqMan MicroRNA RT kit and TaqMan MicroRNA assays (hsa-miR-26a, assay ID 000405; hsa-miR-101, assay ID 002253; hsa-miR-128a, assay ID 002216; RNU6B, assay ID 001093) (Applied Biosystems, Foster City, CA, USA) in accordance with the manufacturer's instructions. Each PCR reaction mixture contained 10 μL of LightCycler 480 probes Master Mix, 4 μL of nuclease-free water, 1 μL of 20X specific PCR primer, and 5 μL of RT product. The thermal cycler was programmed as follows: 95°C for 5 min, 40 cycles of 95°C for 15 sec, and 60°C for 60 sec. Using the comparative CT method, we used an endogenous control (RNU6B) to normalize the expression levels of target micro-RNA by correcting differences in the amount of RNA loaded into qPCR reactions.

Western blot analysis and antibodies

Western blot analysis was performed as described previously.[28] The analysis was performed using antibodies to EZH2 and Histone H3 (Cell Signaling Technology, Danvers, MA, USA), phospho EZH2 (Ser21) (Bethyl Laboratories, Montgomery, TX, USA), H3K27me3, dimethylated H3K27 (H3K27me2), monomethylated H3K27 (H3K27me1) (Millipore, Temecula, CA, USA), and β-actin (Sigma, St. Louis, MO, USA).

Immunohistochemistry

Immunohistochemical staining for EZH2 and H3K27me3 was performed on formalin-fixed, paraffin-embedded lymph node samples from lymphoma-type ATL patients and follicular lymphoma patients as a control. The deparaffinized slides were pretreated with DAKO Target Retrieval Solution, pH 9 (DAKO Japan, Tokyo, Japan), and heated in a water bath at 95°C for 40 min. For all stains, the endogenous peroxidase was quenched using 3% H_2O_2 for 15 min. Sections were then placed in 0.5% non-fat dry milk for 30 min at room temperature. The primary antibodies used were anti-EZH2 antibody (BD Biosciences, San Jose, CA, USA) and anti-H3K27me3 antibody (Cell Signaling Technology, Boston, MA, USA), and were applied at 1:50 dilution and 1:100 dilution, respectively. They were allowed to react for 1 h at room temperature, and then the DAKO EnVision™ + Dual Link System-HRP (DAKO Japan, Tokyo, Japan) was applied using diaminobenzidine as the chromogen, following the manufacturer's protocol.

Sensitivity of adult T-cell leukemia/lymphoma cell lines to DZNep and PS (LBH589)

DZNep was synthesized by one of the authors (VEM). Cells were treated with different concentrations of DZNep for 72 h and the cell proliferation status was evaluated by an MTS assay using a Cell Titer 96® AQueos Cell Proliferation Assay kit (Promega, Madison, WI, USA) in accordance with the manufacturer's instructions. To analyze the synergistic effect of combined treatment with DZNep and PS (LBH589) (kindly provided by Novartis Pharma AG, Basel, Switzerland), cells were treated with DZNep (0.3-5.0 μM) and PS (LBH589) (3-50 nM) for 48 h. After the cell proliferation status was evaluated by an MTS assay, the combination index (CI) for each drug combination was obtained by determining the median dose effect of Chou and Talalay using the CI equation within the commercially available software Calcusyn (Biosoft).[29] CI<1, CI=1, and CI>1 indicate synergism, additive effect, and antagonism, respectively. Cell viability represents the value relative to that of the control culture without these agents.

Results

Microarray analysis shows increased EZH2 and/or RYBP transcripts in adult T-cell leukemia/lymphoma cells

In a comparative microarray analysis of primary ATL samples, we focused on investigating PcG protein genes, *EZH2*, *RYBP*, *BMI-1*, and *CBX7*, in the present study because ATL cells show many aberrantly hypermethylated DNA sequences.[30] ATL cells expressed significantly higher levels of *EZH2* and *RYBP* transcripts than $CD4^+$ T cells from healthy adults (Figure 1A and B). In addition, there was a difference between ATL subtypes in these expressions, and cells from the acute type showed significantly higher levels of these transcripts than the cells from the chronic type. When patients were separated into two groups consisting of those with high expression and those with low expression, the group with high *EZH2* or high *RYBP* transcript showed significantly shorter survival than the respective low-expression groups (Figure 1E and F), indicating that high *EZH2* and/or *RYBP* expression is associated with aggressive clinical behavior. Convincingly, there was a trend toward accumulation of acute-type ATL in the high *EZH2* or the high *RYBP* expression group: 14 cases of acute type and 6 cases of chronic type in the high *EZH2* group, 7 cases of acute type and 13 cases of chronic type in the low *EZH2* group, 14 cases of acute type and 6 cases of chronic type in the high RYBP group, and 7 cases of acute type and 13 cases of chronic type in the low RYBP group. BMI1 is known to down-regulate the expression of *p14ARF/p16INK4A* and lead to neoplastic transformation.[31] Chromobox 7 (CBX7), a component of the PRC1, is also known to repress the transcription of *p14ARF/p16INK4A*.[32] Since inactivation of *p14ARF/p15INK4B/p16INK4A* genes is one of the key events in ATL progression, expression of *BMI-1* and/or *CBX7* transcript was expected to be elevated in acute-type ATL cells. There was, however, no difference in these expressions between ATL subtypes or even between ATL cells and normal $CD4^+$ T cells (Figure 1C and D). There was no difference in survival for different *BMI-1* or *CBX7* expression levels (Figure 1G and H).

Confirmation of increased EZH2 and/or RYBP transcripts by quantitative real-time RT-PCR

For confirmation of the results of microarray analysis, we quantified the transcripts of the PcG protein genes including *EZH2* and *RYBP* by qRT-PCR using another set of samples from ATL patients, healthy adults, HTLV-1 carriers, and hematologic cell lines including ATL cell lines. In accordance with the results of microarray analysis, *EZH2* and *RYBP* transcripts were increased in primary ATL cells compared with those in the cells from healthy adults and HTLV-1 carriers, with statistically significantly higher val-

ues in *EZH2* in terms of both absolute copy number per 25 ng of total RNA and normalized expression level (*Online Supplementary Figure S1A, a, B, b*). *RBBP4* was significantly higher in primary ATL cells than in the cells from healthy adults and HTLV-1 carriers in terms of normalized expression level (*Online Supplementary Figure S1 C, c*). In contrast, there was no difference in *BMI1*, *YY1*, and *EED* expressions among these groups, although some patients showed very high *BMI1* expression (*Online Supplementary Figure S1D, d, E, e, F, f*). Similarly to primary ATL cells, some ATL cell lines showed high *EZH2* expression in terms of absolute copy number per 25 ng of total RNA (*Online Supplementary Figure S1A*).

EZH2 protein expression with trimethylation of H3K27 is characteristic in adult T-cell leukemia/lymphoma cells

We then examined EZH2 and RYBP at the protein level by Western blotting. A 98-kDa band for EZH2 protein and a 32-kDa band for RYBP protein were detected in all primary ATL samples irrespective of subtype, but they were hardly detected in cells from healthy adults and HTLV-1 carriers (Figure 2A, *Online Supplementary Figure S2*, and *data not shown*). ATL cell lines and acute T-lymphoblastic leukemia cell lines also showed intense EZH2 bands. The serine-threonine kinase Akt phosphorylates EZH2 at serine 21 and suppresses its methyltransferase activity by impeding EZH2 binding to histone H3, which results in a decrease in lysine 27 trimethylation.[33] EZH2 of ATL cells was not phosphorylated and was in its active form (Figure 2A). In fact, most primary ATL samples showed the band for H3K27me3, while the cells from healthy adults lacked the band (Figure 2B). As it is known that EZH2 plays a crucial role in trimethylation but not in dimethylation or monomethylation, the bands for H3K27me2 and H3K27me1 were detected in all samples examined, but the band for H3K27me3 was limited in primary ATL cells and ATL cell lines LMY1 and KOB that showed an intense EZH2 band with a faint phosphorylated EZH2 band (Figure 2A and B). In contrast, EZH2 was strongly phosphorylated in ATL cell lines ST1, SO4, KK1, and acute T-lymphoblastic leukemia cell lines Jurkat and MOLT4, and these cell lines hardly showed the band for H3K27me3. Collectively, these results indicate that ATL cells express

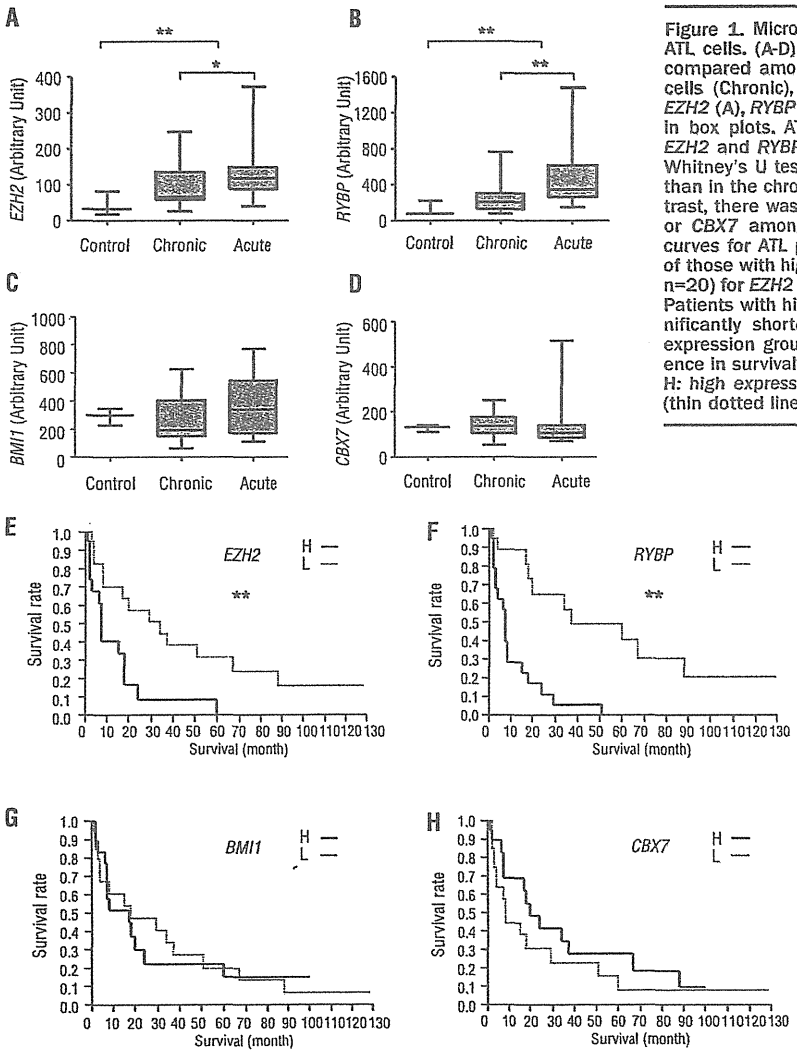

Figure 1. Microarray analysis of gene expression in primary ATL cells. (A-D) Expression levels of PcG protein genes were compared among normal CD4+ T cells (Control), chronic ATL cells (Chronic), and acute ATL cells (Acute), and results of *EZH2* (A), *RYBP* (B), *BMI1* (C), and *CBX7* (D) are demonstrated in box plots. ATL cells showed significantly higher levels of *EZH2* and *RYBP* transcripts than normal CD4+ T cells (Mann-Whitney's U test), with a higher expression in the acute type than in the chronic type (Mann-Whitney's U test) (A, B). In contrast, there was no statistical difference in the level for *BMI1* or *CBX7* among these groups (C, D). (E-H) Overall survival curves for ATL patients separated into two groups consisting of those with high expression (H, n=20) and low expression (L, n=20) for *EZH2* (E), *RYBP* (F), *BMI1* (G), or *CBX7* (H) are shown. Patients with high *EZH2* or high *RYBP* expression showed significantly shorter survival than those in corresponding low expression groups (log rank test) (E, F). There was no difference in survival for different *BMI1* or *CBX7* expressions (G, H). H: high expression group (bold line), L: low expression group (thin dotted line). $*P<0.05$, $**P<0.01$

functionally active EZH2, and as a result, their H3K27 are trimethylated, and that ATL cell lines LMY1 and KOB preserve this characteristic of primary ATL cells.

Immunohistochemical confirmation of the expression of EZH2 and H3K27me3 in lymph nodes

We next used lymph nodes from lymphoma-type ATL patients for immunohistochemical evaluation of EZH2 expression and H3K27me3. In agreement with the results of Western blotting, all ATL lymph nodes from 7 patients were strongly positive for both EZH2 and H3K27me3 without exception in their nuclear staining (*Online Supplementary Figure S3* and *data not shown*), suggesting that overexpression of EZH2 with H3K27me3 is a common feature of ATL cells irrespective of ATL subtypes. In contrast, in lymph nodes from 5 follicular lymphoma patients, only a few cells were positive for EZH2 with some variation among patients and most cells were negative for H3K27me3 (*Online Supplementary Figure S3* and *data not shown*).

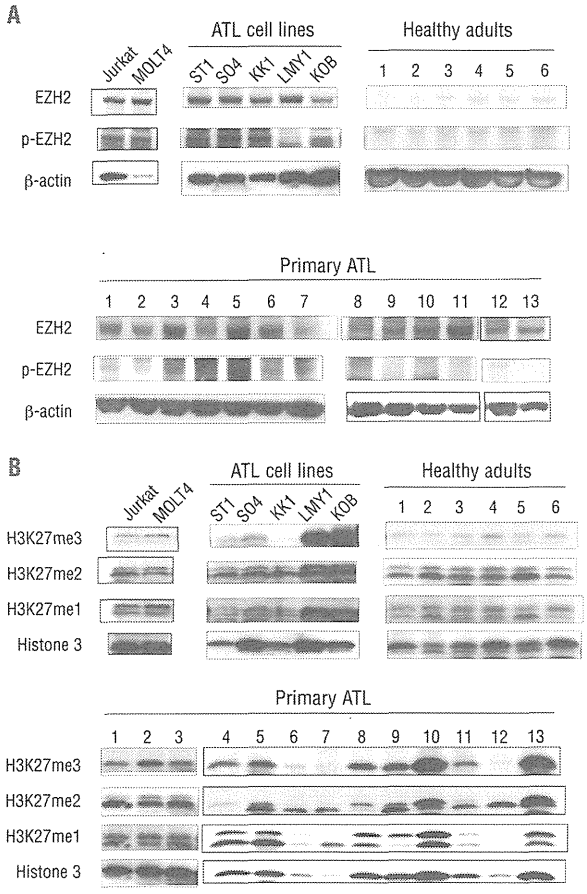

Figure 2. EZH2 protein expression and histone methylation. (A) Western blot analysis for EZH2 protein was performed on primary ATL cells, cells from healthy adults, and ATL cell lines. Primary ATL cells showed a clear 98-kDa band for EZH2 with the absence or presence of faint bands for phosphorylated EZH2 (p-EZH2). Cells from healthy adults hardly showed these bands. ATL cell lines ST1, SO4, and KK1 showed intense bands for both EZH2 and p-EZH2, but LM-Y1 and KOB cells showed intense bands for EZH2 with the absence of a band for p-EZH2. (B) Western blot analysis for histone methylation status was performed. Only primary ATL cells and LM-Y1 and KOB cell lines showed a clear band for H3K27me3, but others hardly showed the band. Bands for H3K27me2, H3K27me1, and histone H3 were observed in almost all samples examined.

Downregulation of miR-101 and miR-128a may be responsible for increased EZH2 expression

So far, more than 700 miRNAs have been identified in humans, and each miRNA regulates multiple target genes. miR-101 and miR-26a have been shown to be negative regulators of *EZH2* expression and are depressed in several types of cancer cells.[34,35] miR-128a is known to be a negative regulator of *BMI1* and has been reported to be involved in glioma cell proliferation.[36] We quantified these miRNAs in primary ATL cells and cells from HTLV-1 carriers to investigate the mechanism of *EZH2* overexpression. ATL cells showed significantly decreased levels of miR-101 and miR-128a compared with the cells from HTLV-1 carriers (Figure 3A and C). Notably, there were significant inverse correlations between *EZH2* expression and miR-101 expression or *EZH2* expression and miR-128a expression (Figure 3D and E), suggesting that decrease of these miRNAs accounts for the overexpression of *EZH2*. Since genomic loss of miR-101 has been reported in prostate cancer,[34] we performed quantitative genomic PCR for miR-101 in two loci, miR-101-1 (chromosome 1p31) and miR-101-2 (chromosome 9p24). Both loci were preserved in all 10 ATL samples examined (*Online Supplementary Figure S4*). The expression of miR-26a did not, in contrast, differ between ATL cells and cells from HTLV-1 carriers (Figure 3B). Unexpectedly, there was no significant correlation between *BMI1* expression and miR-128a expression (Figure 3F).

Adult T-cell leukemia/lymphoma cells are sensitive to DZNep and PS (LBH589)

We first examined the sensitivity of ATL-related cell lines and acute T-lymphoblastic leukemia cell lines to DZNep, an inhibitor of S-adenosylhomocysteine hydrolase, which has recently been shown to decrease the expression of EZH2 and histone methylation.[22,25] DZNep inhibited the proliferation of these cell lines, at concentrations above 0.5 μM (*Online Supplementary Figure S5A*). In contrast, $CD4^+$ T cells from healthy adults as a normal control were resistant to DZNep even at 5 μM. Notably, although DZNep decreased *EZH2* expression in ST1, SO4, and KK1, it did not decrease but rather increased the expression in KOB, results which were confirmed by Western blot (*Online Supplementary Figure S5B and C*). PS (LBH589) is also known to decrease the level of EZH2 in several types of leukemia cells.[24] One hundred nM of PS (LBH589) decreased *EZH2* expression at both transcript and protein levels in ATL cell lines including KOB and LM-Y1, which showed a similar EZH2 expression profile to that of primary ATL cells, namely, high EZH2 expression with low phosphorylated EZH2 and strong H3K27me3 (*Online Supplementary Figure S5D and E*). We next examined whether these agents show a synergistic effect or just an additive effect. As shown in *Online Supplementary Figure S5F* (upper panel), the cell viabilities of LM-Y1 treated with 25 nM PS (LBH589) or 2.5 μM DZNep were 70% and 87%, respectively. A combination of this setting (LBH:DZNep=1:100) markedly decreased the proportion of viable cells (40%) compared with that of cells treated

with either agent alone. Similarly, cell viabilities of KOB treated with 25 nM PS (LBH589), 2.5 μM DZNep, or a combination of these agents were 86%, 93%, and 48%, respectively. By calculating CI according to the method of Chou and Talalay,[29] we found a strong synergistic antiproliferative effect in both cell lines (*Online Supplementary Figure S5F*, lower panel).

Discussion

EZH2 is a critical component of PRC2, which mediates epigenetic gene silencing through trimethylation of H3K27.[37,38] EED and SUZ12 are also required for the exhibition of methyltransferase activity and for the localization of this complex to target genes.[39] In an analysis of genome-wide H3K27 methylation in aggressive prostate cancer tissues, a significant subset of the target genes were also targets in embryonic stem cells, suggesting that the mechanism for gene silencing used to maintain stem cell renewal is converted into oncogenesis.[40] Ectopic expression of EZH2 is capable of providing a proliferative advantage to primary cells, and its gene locus is amplified in primary tumors.[41] Indeed, increased EZH2 expression has been reported in several types of cancer cells, and its clinical significance is extensively studied in prostate cancer.[42] Amounts of both *EZH2* transcript and EZH2 protein were elevated in metastatic prostate cancer; in addition, clinically localized prostate cancers that express higher concentrations of *EZH2* showed a poorer prognosis. An association of increased EZH2 expression with poor prognosis has also been reported in other solid tumors. Currently, however, there are only limited reports describing EZH2 expression in hematologic malignancies.

In the present study, we showed for the first time that EZH2 was over-expressed in ATL cells, and that the increased EZH2 was not phosphorylated and was in its active form. The increased EZH2 seemed to exhibit histone methyltransferase activity *in vivo*, as supported by the results that ATL cells from both peripheral blood and lymph nodes were strongly positive for H3K27me3. Since EZH2 was almost undetectable in cells from healthy adults and HTLV-1 carriers, it is likely that deregulation of PRC2 caused by over-expressed EZH2 is involved in the early steps of ATL oncogenesis. Meanwhile, ATL patients with high EZH2 expression showed shorter survival than patients with low EZH2 expression, indicating that increased EZH2 also plays a role in the process of ATL progression. It has been reported that genes methylated in cancer cells are specifically packaged with nucleosomes containing H3K27.[43] However, there are only a few studies that actually examined H3K27me3 in primary tumor cells or tissues. In one such study, H3K27me3 expression was unexpectedly lower in breast, ovarian, and pancreatic cancers than in corresponding normal tissues, although it has been reported that there are increased levels of H3K27me3 in breast cancer cell lines.[44,45] We do not have an adequate explanation for these conflicts at present, but there may be some differences in the process of oncogenesis between solid tumors and hematologic malignancies.

The mechanism of the overexpression of EZH2 in tumors remains largely unknown. miRNAs regulate gene expression and play important roles in cellular differentiation and embryonic stem cell development. Recently, two miRNAs, miR-101 and miR-26a, were found to repress *EZH2* expression. The expression of miR-101 decreases in parallel with an increase in *EZH2* expression during progression in prostate tumors.[34] In addition to these miRNAs, we examined miR-128a, which has been shown to repress *BMI1* expression in glioblastoma, because overexpression of *BMI-1* is associated with the development of malignant lymphoma.[31,36] ATL cells showed a decreased level of miR-

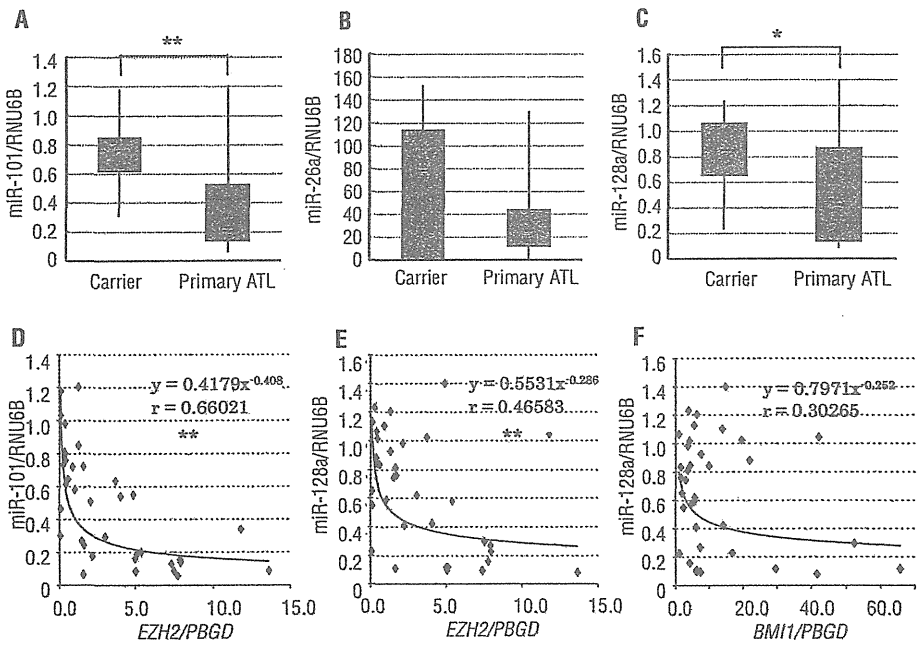

Figure 3. Quantitative real-time RT-PCR for miRNAs. (A-C) Expressions of miR-101 (A), miR-26a (B), and miR-128a (C) were compared between ATL patients and HTLV-1 carriers. Primary ATL cells showed significantly lower levels of miR-101 and miR-128a (Mann-Whitney's U test) compared with the cells from HTLV-1 carriers (A, C). There was no significant difference in miR-26a expression between the two groups (B). (D, E, F) Correlation between miRNA and *EZH2* or *BMI1* expression was examined. There were significant inverse correlations between normalized *EZH2* expression and miR-101 expression (D) or between normalized *EZH2* expression and miR-128a expression (E) (Spearman's correlation coefficient). In contrast, there was no correlation between normalized *BMI1* expression and miR-128a expression (F). $*P<0.05$, $**P<0.01$

101 expression compared with the cells from HTLV-1 carriers, which is not caused by genomic loss of the *miR-101* gene, in contrast to prostate cancer.[34] Moreover, there was a clear inverse correlation between *EZH2* expression and miR-101 expression, suggesting that increased *EZH2* is caused by the decrease in miR-101 expression. Although currently there is no report indicating an association of miR-128a with *EZH2* expression, miR-128a showed exactly the same pattern as miR-101, suggesting that the decrease in miR-128a also participates in *EZH2* overexpression in ATL. By analyzing the 3'-UTR sequence of *EZH2*, it has recently been shown that there are two predicted miR-101 target sites and one predicted miR-26a target site in the 3'-UTR of EZH2.[46] We performed a similar analysis and found that there was also a potential target site for miR-128a near one of the miR-101 target sites (*Online Supplementary Figure S6*). miR-26a was not decreased in ATL cells, and there was no correlation between miR-26a expression and *EZH2* expression or miR-128a expression and *BMI1* expression. The association of miR-26a with *EZH2* was found in normal cell differentiation as a physiological phenomenon but not in tumor cells. The miRNAs used to regulate normal development and differentiation may be different from those used for the development of tumors. Another possible explanation for the mechanism of increased *EZH2* expression in ATL is inactivation of *p14ARF/p15INK4B/p16INK4A* tumor suppressor genes, which frequently occurs in ATL.[14,15,19,20] EZH2 is a molecule downstream of the pRB-E2F pathway, and inactivation of these genes allows E2F to be released from pRB, which results in the upregulation of *EZH2* expression.[43] Several recent reports indicate that EZH2 functions to repress the expression of *p14ARF/p15INK4B/p16INK4A*; therefore, increased EZH2 may be used to further decrease the expression of *p14ARF/p15INK4B/p16INK4A*.[47] Since somatic mutations altering EZH2 (Tyr641) have recently been reported in follicular and diffuse large B-cell lymphomas of germinal-center origin,[48] we performed a similar analysis in 10 primary ATL samples. There were however no such mutations (*Online Supplementary Figure S7*).

ATL is quite resistant to antineoplastic agents and the median survival time of those with the aggressive subtypes is only 13 months, even in a recent multicenter clinical trial.[49] Since high EZH2 expression with H3K27me3 seems to be an essential component for the initiation and promotion of cell proliferation in ATL, we searched for the possibility of therapeutic strategies targeting EZH2. We examined the sensitivity of ATL cells to agents that have been shown to inhibit *EZH2* expression and histone methylation. DZNep is a carbocyclic analog of adenosine synthesized more than 20 years ago as an inhibitor of S-adenosylhomocysteine hydrolase, which has therapeutic potential as an anticancer or antiviral drug.[21] DZNep has recently aroused interest for its unique features; it decreases the expressions of *EZH2*, *SUZ12*, and *EED* with inhibition of H3K27 methylation and induces apoptosis in cancer cells but not in normal cells.[22,23] ATL cell lines were sensitive to DZNep and their cell proliferation was attenuated at one-tenth of the concentration used in these studies. More interestingly, DZNep showed no toxicity to normal $CD4^+$ T cells as a normal control. Acute T-lymphoblastic leukemia cell lines showed similar sensitivities to DZNep, which may indicate that DZNep exerts general toxicity to leukemia and lymphoma cells not necessarily associated with histone modification. Indeed, although DZNep rather increased EZH2 expression in KOB cells, this cell line was equally sensitive as other cell lines to DZNep. HDAC inhibitor PS (LBH589) is an effective agent for cutaneous T-cell lymphoma and induced complete remission in 2 of 9 patients involved in a phase I clinical trial.[50] More interestingly, it has been reported recently that combined use of DZNep and PS (LBH589) yielded more depletion of EZH2 and induced more apoptosis of leukemia cells, but not normal CD34 (+) bone marrow progenitor cells.[51] In the present study, we showed that the combination of DZNep and PS (LBH589) exhibited a synergistic effect in killing ATL cells. Thus, epigenetic therapy by the combined use of these agents that inhibit histone methylation could lead to a breakthrough in the treatment of aggressive ATL.

Authorship and Disclosures

The information provided by the authors about contributions from persons listed as authors and in acknowledgments is available with the full text of this paper at www.haematologica.org.

Financial and other disclosures provided by the authors using the ICMJE (www.icmje.org) Uniform Format for Disclosure of Competing Interests are also available at www.haematologica.org.

References

1. Sparmann A, van Lohuizen M. Polycomb silencers control cell fate, development and cancer. Nat Rev Cancer. 2006;6(11):846-56.
2. Lee TI, Jenner RG, Boyer LA, Guenther MG, Levine SS, Kumar RM, et al. Control of developmental regulators by Polycomb in human embryonic stem cells. Cell. 2006;125(2):301-13.
3. Kamminga LM, Bystrykh LV, de Boer A, Houwer S, Douma J, Weersing E, et al. The Polycomb group gene Ezh2 prevents hematopoietic stem cell exhaustion. Blood. 2006;107(5):2170-9.
4. van Lohuizen M, Tijms M, Voncken JW, Schumacher A, Magnuson T, Wientjens E. Interaction of mouse polycomb-group (Pc-G) proteins Enx1 and Enx2 with Eed: Indication for separate Pc-G complexes. Mol Cell Biol. 1998;18(6):3572-9.
5. Satijn DP, Hamer KM, den Blaauwen J, Otte AP. The Polycomb group protein EED interacts with YY1, and both proteins induce neural tissue in Xenopus embryos. Mol Cell Biol. 2001;21(4):1360-9.
6. van der Vlag J, Otte AP. Transcriptional repression mediated by the human polycomb-group protein EED involves histone deacetylation. Nat Genet. 1999;23(4):474-8.
7. Vire E, Brenner C, Deplus R, Blanchon L, Fraga M, Didelot C, et al. The Polycomb group protein EZH2 directly controls DNA methylation. Nature. 2006;439(7078):871-4.
8. Cao R, Zhang Y. The functions of E(Z)EZH2-mediated methylation of lysine 27 in histoneH3. Curr Opin Genet Dev. 2004;14(2):155-64.
9. Widschwendter M, Fiegl H, Egle D, Mueller-Holzner E, Spizzo G, Marth C, et al. Epigenetic stem cell signature in cancer. Nat Genet. 2007;39(2):157-8.
10. Simon JA, Lange CA. Roles of the EZH2 histone methyltransferase in cancer epigenetics. Mutat Res. 2008;647(1-2):21-9.
11. Uchiyama T, Yodoi J, Sagawa K, Takatsuki K, Uchino H. Adult T-cell leukemia: clinical and hematologic features of 16 cases. Blood. 1977;50(3):481-92.
12. Yoshida M, Seiki M, Yamaguchi K, Takatsuki K. Monoclonal integration of human T-cell leukemia provirus in all primary tumors of adult T-cell leukemia suggests causative role of human T-cell leukemia virus in the disease. Proc Natl Acad Sci USA. 1984;81(8):2534-7.
13. Shimoyama M and members of the Lymphoma Study Group (1984-1987):

Diagnostic criteria and classification of clinical subtypes of adult T-cell leukaemia-lymphoma. A report from the Lymphoma Study Group (1984-1987). Br J Haematol. 1991;79(3):428-37.
14. Hatta Y, Hirama T, Miller CW, Yamada Y, Tomonaga M, Koeffler HP. Homozygous deletions of p15 (MTS2) and p16 (CDKN2/MTS1) genes in adult T-cell leukemia. Blood. 1995;85(10):2699-704.
15. Yamada Y, Hatta Y, Murata K, Sugawara K, Ikeda S, Mine M, et al. Deletions of p15 and/or p16 genes as a poor-prognosis factor in adult T-cell leukemia. J Clin Oncol. 1997;15(5):1778-85.
16. Nagai H, Kinoshita T, Imamura J, Murakami Y, Hayashi K, Mukai K, et al. Genetic alteration of p53 in some patients with adult T-cell leukemia. Jpn J Cancer Res. 1991;82(12):1421-7.
17. Sakashita A, Hattori T, Miller CW, Suzushima H, Asou N, Takatsuki K, et al. Mutations of the p53 gene in adult T-cell leukemia. Blood. 1992;79(2):477-80.
18. Tawara M, Hogerzeil SJ, Yamada Y, Takasaki Y, Soda H, Hasegawa H, et al. Impact of p53 aberration on the progression of adult T-cell leukemia/lymphoma. Cancer Lett. 2006;234(2):249-55.
19. Kohno T, Yamada Y, Tawara M, Takasaki Y, Kamihira S, Tomonaga M, et al. Inactivation of p14ARF as a key event for the progression of adult T-cell leukemia/lymphoma. Leuk Res. 2007;31(12):1625-32.
20. Nosaka K, Maeda M, Tamiya S, Sakai T, Mitsuya H, Matsuoka M. Increasing methylation of the CDKN2A gene is associated with the progression of adult T-cell leukemia. Cancer Res. 2000;60(4):1043-8.
21. Glazer RI, Hartman KD, Knode MC, Richard MM, Chiang PK, Tseng CK, et al. 3-Deazaneplanocin: a new and potent inhibitor of S-adenosylhomocysteine hydrolase and its effects on human promyelocytic leukemia cell line HL-60. Biochem Biophys Res Commun. 1986;135 (2):688-94.
22. Miranda TB, Cortez CC, Yoo CB, Liang G, Abe M, Kelly TK, et al. DZNep is a global histone methylation inhibitor that reactivates developmental genes not silenced by DNA methylation. Mol Cancer Ther. 2009;8(6):1579-88.
23. Tan J, Yang X, Zhuang L, Jiang X, Chen W, Lee PL, et al. Pharmacologic disruption of Polycomb-repressive complex 2-mediated gene repression selectively induces apoptosis in cancer cells. Genes Dev. 2007;21(9): 1050-63.
24. Fiskus W, Pranpat M, Balasis M, Herger B, Rao R, Chinniyan A, et al. Histone deacetylase inhibitors deplete EZH2 and associated Polycomb Repressive Complex 2 proteins with attenuation of HOXA9 and MEIS1 and loss of survival of human acute leukemia cells. Mol Cancer Ther. 2006;5 (12):3096-104.
25. Choi YL, Tsukasaki K, O'Neill MC, Yamada Y, Onimaru Y, Matsumoto K, et al. A genomic analysis of adult T-cell leukemia. Oncogene. 2007;26(8):1245-55.
26. Yamada Y, Ohmoto Y, Hata T, Yamamura M, Murata K, Tsukasaki K, et al. Features of the cytokines secreted by adult T cell leukemia (ATL) cells. Leuk Lymphoma. 1996;21(5-6):443-7.
27. Choi YL, Makishima H, Ohashi J, Yamashita Y, Ohki R, Koinuma K, et al. DNA microarray analysis of natural killer cell-type lymphoproliferative disease of granular lymphocytes with purified CD3(-) CD56(+) fractions. Leukemia. 2004;18(3): 556-65.
28. Hasegawa H, Yamada Y, Komiyama K, Hayashi M, Ishibashi M, Sunazuka T, et al. A novel natural compound, a cycloanthranilylproline derivative (Fuligocandin B), sensitizes leukemia cells to apoptosis induced by tumor necrosis factor related apoptosis-inducing ligand (TRAIL) through 15-deoxy-Delta 12, 14 prostaglandin J2 production. Blood. 2007;110(5):1664-74.
29. Chou TC, Talalay P. Quantitative analysis of dose-effect relationships: the combined effects of multiple drugs or enzyme inhibitors. Adv Enzyme Regul. 1984;22:27-55.
30. Yasunaga J, Taniguchi Y, Nosaka K, Yoshida M, Satou Y, Sakai T, et al. Identification of aberrantly methylated genes in association with adult T-cell leukemia. Cancer Res. 2004;64(17):6002-9.
31. Jacobs JJ, Kieboom K, Marino S, DePinho RA, van Lohuizen M. The oncogene and Polycomb-group gene bmi-1 regulates cell proliferation and senescence through the ink4a locus. Nature. 1999;397(6715):164-8.
32. Scott CL, Gil J, Hernando E, Teruya-Feldstein J, Narita M, Martinez D, et al. Role of the chromobox protein CBX7 in lymphomagenesis. Proc Natl Acad Sci USA. 2007;104(13):5389-94.
33. Cha TL, Zhou BP, Xia W, Wu Y, Yang CC, Chen CT, et al. Akt-mediated phosphorylation of EZH2 suppresses methylation of Lysine 27 in histone H3. Science. 2005;310(5746):306-10.
34. Varambally S, Cao Q, Mani RS, Shankar S, Wang X, Ateeq B, et al. Genomic loss of microRNA-101 leads to overexpression of histone methyltransferase EZH2 in cancer. Science. 2008;322(5908):1695-6.
35. Sander S, Bullinger L, Klapproth K, Fiedler K, Kestler HA, Barth TF, et al. MYC stimulates EZH2 expression by repression of its negative regulator miR-26a. Blood. 2008; 112(10):4202-12.
36. Godlewski J, Nowicki MO, Bronisz A, Williams S, Otsuki A, Nuovo G, et al. Targeting of the Bmi-1 oncogene/stem cell renewal factor by microRNA-128 inhibits glioma proliferation and self-renewal. Cancer Res. 2008;68(22):9125-30.
37. Cao R, Wang L, Wang H, Xia L, Erdjument-Bromage H, Tempst P, et al. Role of histone H3 lysine 27 methylation in Polycomb-group silencing. Science. 2002;298(5595): 1039-43.
38. Czermin B, Melfi R, McCabe D, Seitz V, Imhof A, Pirrotta V. Drosophila enhancer of Zeste/ESC complexes have a histone H3 methyltransferase activity that marks chromosomal Polycomb sites. Cell. 2002;111(2): 185-96.
39. Cao R, Zhang YI. SUZ12 is required for both the histone methyltransferase activity and the silencing function of the EED-EZH2 complex. Mol Cell. 2004;15(1):57-67.
40. Yu J, Yu J, Rhodes DR, Tomlins SA, Cao X, Chen G, et al. A polycomb repression signature in metastatic prostate cancer predicts cancer outcome. Cancer Res. 2007; 67(22):10657-63.
41. Bracken AP, Pasini D, Capra M, Prosperini E, Colli E, Helin K. EZH2 is downstream of the pRB-E2F pathway, essential for proliferation and amplified in cancer. EMBO J. 2003;22(20):5323-35.
42. Varambally S, Dhanasekaran SM, Zhou M, Barrette TR, Kumar-Sinha C, Sanda MG, et al. The polycomb group protein EZH2 is involved in progression of prostate cancer. Nature. 2002;419(6907):624-9.
43. Schlesinger Y, Straussman R, Keshet I, Farkash S, Hecht M, Zimmerman J, et al. Polycomb-mediated methylation of Lys27 of histone H3 pre-marks genes for de novo methylation in cancer. Nat Genet. 2007;39 (2):232-6.
44. Wei Y, Xia W, Zhang Z, Liu J, Wang H, Adsay NV, et al. Loss of trimethylation at lysine 27 of histone H3 is a predictor of poor outcome in breast, ovarian, and pancreatic cancers. Mol Carcinog. 2008;47 (9):701-6.
45. Sun F, Chan E, Wu Z, Yang X, Marquez VE, Yu Q. Combinatorial pharmacologic approaches target EZH2-mediated gene repression in breast cancer cells. Mol Cancer Ther. 2009;8(12):3191-202.
46. Cao P, Deng Z, Wan M, Huang W, Cramer SD, Xu J, et al. MicroRNA-101 negatively regulates Ezh2 and its expression is modulated by androgen receptor and HIF-1alpha/HIF-1beta. Mol Cancer. 2010;9: 108.
47. Bracken AP, Kleine-Kohlbrecher D, Dietrich N, Pasini D, Gargiulo G, Beekman C, et al. The polycomb group proteins bind throughout the INK4A-ARF locus and are disassociated in senescent cells. Genes Dev. 2007;21(5):525-30.
48. Morin RD, Johnson NA, Severson TM, Mungall AJ, An J, Goya R, et al. Somatic mutations altering EZH2 (Tyr641) in follicular and diffuse large B-cell lymphomas of germinal-center origin. Nat Genet. 2010; 42(2):181-5.
49. Yamada Y, Tomonaga M, Fukuda H, Hanada S, Utsunomiya A, Tara M, et al. A new G-CSF-supported combination chemotherapy, LSG15, for adult T-cell leukaemia-lymphoma: Japan Clinical Oncology Group Study 9303. Br J Haematol. 2001;113(2):375-82.
50. Ellis L, Pan Y, Smyth GK, George DJ, McCormack C, Williams-Truax R, et al. Histone deacetylase inhibitor panobinostat induces clinical responses with associated alterations in gene expression profiles in cutaneous T-cell lymphoma. Clin Cancer Res. 2008;14(14):4500-10.
51. Fiskus W, Wang Y, Sreekumar A, Buckley KM, Shi H, Jillella A, et al. Combined epigenetic therapy with the histone methyltransferase EZH2 inhibitor 3-deazaneplanocin A and the histone deacetylase inhibitor panobinostat against human AML cells. Blood. 2009;114(13):2733-43.

THE JOURNAL OF IMMUNOLOGY

HTLV-1 bZIP Factor–Specific CD4 T Cell Responses in Adult T Cell Leukemia/Lymphoma Patients After Allogeneic Hematopoietic Stem Cell Transplantation

Tomoko Narita, Takashi Ishida, Ayako Masaki, Susumu Suzuki, Asahi Ito, Fumiko Mori, Tomiko Yamada, Masaki Ri, Shigeru Kusumoto, Hirokazu Komatsu, Yasuhiko Miyazaki, Yoshifusa Takatsuka, Atae Utsunomiya, Akio Niimi, Shinsuke Iida and Ryuzo Ueda

J Immunol published online 20 December 2013
http://www.jimmunol.org/content/early/2013/12/20/jimmunol.1301952

The Journal of Immunology is published twice each month by The American Association of Immunologists, Inc., 9650 Rockville Pike, Bethesda, MD 20814-3994.

Print ISSN: 0022-1767 Online ISSN: 1550-6606.

Published December 20, 2013, doi:10.4049/jimmunol.1301952

HTLV-1 bZIP Factor–Specific CD4 T Cell Responses in Adult T Cell Leukemia/Lymphoma Patients After Allogeneic Hematopoietic Stem Cell Transplantation

Tomoko Narita,* Takashi Ishida,* Ayako Masaki,* Susumu Suzuki,*,† Asahi Ito,* Fumiko Mori,* Tomiko Yamada,* Masaki Ri,* Shigeru Kusumoto,* Hirokazu Komatsu,* Yasuhiko Miyazaki,‡ Yoshifusa Takatsuka,§ Atae Utsunomiya,§ Akio Niimi,* Shinsuke Iida,* and Ryuzo Ueda†

We document human T lymphotropic virus type 1 (HTLV-1) bZIP factor (HBZ)-specific CD4 T cell responses in an adult T cell leukemia/lymphoma (ATL) patient after allogeneic hematopoietic stem cell transplantation (HCT) and identified a novel HLA-DRB1*15:01–restricted HBZ-derived naturally presented minimum epitope sequence, RRRAEKKAADVA (HBZ114–125). This peptide was also presented on HLA-DRB1*15:02, recognized by CD4 T cells. Notably, HBZ-specific CD4 T cell responses were only observed in ATL patients after allogeneic HCT (4 of 9 patients) and not in nontransplanted ATL patients (0 of 10 patients) or in asymptomatic HTLV-1 carriers (0 of 10 carriers). In addition, in one acute-type patient, HBZ-specific CD4 T cell responses were absent in complete remission before HCT, but they became detectable after allogeneic HCT. We surmise that HTLV-1 transmission from mothers to infants through breast milk in early life induces tolerance to HBZ and results in insufficient HBZ-specific T cell responses in HTLV-1 asymptomatic carriers or ATL patients. In contrast, after allogeneic HCT, the reconstituted immune system from donor-derived cells can recognize virus protein HBZ as foreign, and HBZ-specific immune responses are provoked that contribute to the graft-versus-HTLV-1 effect. *The Journal of Immunology*, **2014, 192: 000–000.**

Adult T cell leukemia/lymphoma (ATL) is a distinct hematologic malignancy caused by human T lymphotropic virus type 1 (HTLV-1) (1, 2). ATL is resistant to conventional chemotherapeutic agents, and only limited treatment options are available (3). Although early efforts using myeloablative chemoradiotherapy together with autologous hematopoietic stem cell rescue for ATL were associated with a high incidence of relapse and fatal toxicities (4), allogeneic hematopoietic stem cell transplantation (HCT) has been explored as a promising alternative treatment, achieving long-term remission in a proportion of patients with ATL (5, 6). The potential benefit of allogeneic HCT for ATL patients is considered to be due to the high immunogenicity of HTLV-1–infected cells (7–12), which was associated with the existence of posttransplant graft-versus-HTLV-1 and/or graft-versus-ATL effects (13, 14).

HTLV-1 was the first retrovirus to be directly associated with a human malignancy (15, 16), and ~20 million people worldwide are estimated to be infected with this virus (17). Among the HTLV-1 regulatory and accessory genes, *Tax* transforms rodent cells and immortalizes human primary T cells (18–20). In addition, Tax-transgenic mice develop spontaneous tumors (21–24). Another HTLV-1 component gene, *HBZ*, promotes the proliferation of ATL cells (25). Transgenic mice expressing HTLV-1 bZIP factor (HBZ) in their CD4 T cells share many symptoms and immunological features with HTLV-1–infected humans (26). Thus, both *Tax* and *HBZ* are thought to play critical roles in ATL oncogenesis, but there is a marked contrast between them in their expression profiles in primary ATL cells: HBZ expression is constitutive whereas Tax expression is frequently suppressed or minimal in ATL cells (25, 27, 28). Because immune responses against Tax were reported to be strong (7, 8), impaired Tax expression is thought to lead to a survival advantage for HTLV-1–infected cells in the host (2). These observations raise a simple question as to why the expression of Tax, but not HBZ, is impaired, despite both being HTLV-1–derived Ags seen by the human immune system as foreign. In other words, why is it that only HBZ, but not Tax, is constitutively expressed in ATL cells, although it was reported that HBZ is an immunogenic protein recognized by HBZ-specific CTL clones (29, 30). Although several studies (29–31) have been performed to determine the immunogenicity of HBZ, the precise immunological significance of HBZ in HTLV-1–infected individuals has not been fully established. Therefore, the aim of the current study was to clarify the clinical role of HBZ-specific immune responses in HTLV-1–infected individuals.

*Department of Medical Oncology and Immunology, Nagoya City University Graduate School of Medical Sciences, Nagoya 467-8601, Japan; †Department of Tumor Immunology, Aichi Medical University School of Medicine, Aichi 480-1195, Japan; ‡Department of Hematology, Oita Prefectural Hospital, Oita 870-8511, Japan; and §Department of Hematology, Imamura Bun-in Hospital, Kagoshima 890-0064, Japan

Received for publication July 22, 2013. Accepted for publication November 20, 2013.

This work was supported by grants-in-aid for scientific research (B) (No. 25290058) and scientific support programs for cancer research (No. 221S0001) from the Ministry of Education, Culture, Sports, Science and Technology of Japan, grants-in-aid from the National Cancer Center Research and Development Fund (No. 21-6-3), and H23- Third-Term Comprehensive Control Research for Cancer-general-011 from the Ministry of Health, Labour and Welfare, Japan (all to T.I.). Nagoya City University Graduate School of Medical Sciences received research grant support from Kyowa Hakko Kirin for research carried out by T.I.

Address correspondence and reprint requests to Dr. Takashi Ishida, Department of Medical Oncology and Immunology, Nagoya City University Graduate School of Medical Sciences, 1 Kawasumi, Mizuho-chou, Mizuho-ku, Nagoya, Aichi 467-8601, Japan. E-mail address: itakashi@med.nagoya-cu.ac.jp

Abbreviations used in this article: AC, asymptomatic carrier; ATL, adult T cell leukemia/lymphoma; CR, complete remission; HAM, human T lymphotropic virus type 1–associated myelopathy; HBZ, human T lymphotropic virus type 1 bZIP factor; HCT, hematopoietic stem cell transplantation; HTLV-1, human T lymphotropic virus type 1.

www.jimmunol.org/cgi/doi/10.4049/jimmunol.1301952

Materials and Methods

Primary human cells

Blood samples were obtained from healthy volunteers, HTLV-1 asymptomatic carriers (ACs), and ATL patients. Mononuclear cells were isolated with Ficoll-Paque (Pharmacia, Peapack, NJ). Genotyping of HLA-DR, HLA-DQ, and HLA-DP was performed using an WAKFlow HLA-typing kit (WAKUNAGA Pharmacy, Hiroshima, Japan). Diagnosis and classification of clinical subtypes of ATL were according to the criteria proposed by the Japan Lymphoma Study Group (32). All donors provided informed written consent before sampling, according to the Declaration of Helsinki, and the current study was approved by the institutional ethics committees of Nagoya City University Graduate School of Medical Sciences.

Cell lines

ATN-1, MT-1, TL-Om1, and ATL102 are ATL cell lines; MT-2, MT-4, and TL-Su are HTLV-1–immortalized lines; and K562 is a chronic myelogenous leukemia blast crisis cell line (8, 33). Genotyping of HLA-DR, HLA-DQ, and HAL-DP was performed using a WAKFlow HLA-typing kit.

Expansion of HBZ-specific T cells

PBMCs from ATL patients or HTLV-1 ACs were suspended in RPMI 1640 (Cell Science and Technology Institute, Sendai, Japan) supplemented with 10% human serum and 10 μM synthetic HBZ-derived peptides at a cell concentration of 2×10^6/ml. The peptides were purchased from Invitrogen (Carlsbad, CA). The cell suspension (2×10^6 cells) was cultured at 37°C in 5% CO_2 for 2 d, and an equal volume of RPMI 1640 supplemented with 100 IU/ml IL-2 was added. After subsequent culture for 5 d, an equal volume of ALyS505N (Cell Science and Technology Institute) supplemented with 100 IU/ml IL-2 was added, and the cells were cultured with appropriate medium (ALyS505N with 100 IU/ml IL-2) for an additional 7 d.

Abs and flow cytometry

PerCP-conjugated anti-CD8 mAb (SK1; eBioscience, San Diego, CA) and PE-conjugated anti-CD4 mAb [SFCI12T4D11 (T4); Beckman Coulter, Fullerton, CA] were used. For assessing HLA class II expression, PE-conjugated anti–HLA-DR (G46-6; BD Biosciences, San Jose, CA), anti–HLA-DQ (HLA-DQ1; BioLegend, San Diego, CA), or appropriate isotype-control mAbs were used. For intracellular IFN-γ and TNF-α staining, the expanded cells were cocultured with or without target cells or synthetic peptides at 37°C in 5% CO_2 for 3 h, after which brefeldin A (BD Biosciences) was added at 2 μg/ml. The cells were then incubated for an additional 2 h. Subsequently, they were fixed in 10% formaldehyde and stained with FITC-conjugated anti–IFN-γ (45.15; Beckman Coulter) or allophycocyanin-conjugated anti–TNF-α (MAb11; eBioscience) mAbs with 0.25% saponin for 60 min at room temperature. To determine HLA restriction, HLA-blocking experiments were conducted. The expanded cells were preincubated with 20 μg/ml anti–HLA-DR (L243; BioLegend), 20 μg/ml anti–HLA-DQ (1SPVL3; Beckman Coulter), or appropriate isotype control mAbs (20 μg/ml) at 37°C in 5% CO_2 for 1 h, after which they were stimulated with the peptide or the cell lines (ATN-1 and K562). Cells were analyzed on a FACSCalibur (BD Biosciences) with the aid of FlowJo software (Tree Star, Ashland, OR).

Quantitative RT-PCR

Total RNA was isolated with RNeasy Mini Kits (QIAGEN, Tokyo, Japan). Reverse transcription from the RNA to first-strand cDNA was carried out using High Capacity RNA-to-cDNA Kits (Applied Biosystems, Foster City, CA). *HBZ* and *β-actin* mRNA were amplified using TaqMan Gene Expression Assays with the aid of an Applied Biosystems StepOnePlus. The primer set for *HBZ* was as follows: sense, 5′-TCGACCTGAGCTTTAAACTTACCTAGA-3′ and antisense, 5′-GACACAGGCAAGCATCGAAA-3′. All values given are means of triplicate determinations.

Results

T cell responses against synthetic peptides overlapping by 10 aa and covering the entire sequence of the spliced HBZ protein

Because it was reported that HTLV-1 Tax-specific T cells were induced in some ATL patients after allogeneic HCT (10, 11), we initially tried to expand HBZ-specific T cells using PBMCs from an ATL patient who received allogeneic HCT with reduced-intensity conditioning and has been in complete remission (CR) for >3 y (patient #1 after HCT). PBMCs were stimulated with a mixture of 1 16-mer and 19 20-mer synthetic peptides overlapping by 10 aa and covering the entire sequence of the spliced HBZ protein (peptides number 1–20, Fig. 1), at a concentration of 10 μM each. The expanded cells were analyzed by forward scatter height and side scatter height levels, and the lymphocyte population was determined and plotted to show CD4 and CD8 positivity (Fig. 2A, *left panels*). The expanded CD8 T cells responded weakly to stimulation with these 20 overlapping peptides relative to controls without peptide stimulation, as assessed by IFN-γ production (Fig. 2A, *upper middle panels*) but not TNF-α (Fig. 2A, *lower middle panels*). In contrast, the expanded CD4 T cells responded to stimulation by the 20 overlapping peptides by producing both IFN-γ (Fig. 2A, *upper right panels*) and TNF-α (Fig. 2A, *lower right panels*). Because the response of the stimulated and expanded CD4 T cells was stronger than the CD8 response, we focused on the CD4 T cell response against HBZ in patient #1 after HCT.

PBMCs from this patient (#1 after HCT) were stimulated with a mixture of five overlapping peptides consisting of peptides 1–4, 5–8, 9–12, 13–16, and 17–20 (Fig. 1). The expanded CD4 T cells responded to the peptide mixture 9–12 better than to control (no peptides). They produced both IFN-γ (Fig. 2B, *upper panels*) and TNF-α (Fig. 2B, *lower panels*). The expanded CD4 T cells responded very weakly to the peptide mixtures 13–16 and 17–20 by producing TNF-α but not IFN-γ. No responses were observed against the peptide mixtures 1–4 or 5–8 (Fig. 2B). These data indicate that the epitope of HBZ recognized by CD4 T cells from the patient was present in peptides 9–12, within HBZ aa residues 81–130 (Fig. 1).

Next, PBMCs from the same patient were stimulated with four synthetic peptides: 9, 10, 11, and 12. The expanded CD4 T cells responded to peptide 12 by producing both IFN-γ (Fig. 2C, *upper panels*) and TNF-α (Fig. 2C, *lower panels*). The cells did not respond significantly to the other peptides (9, 10, or 11). These results narrow down the specific epitope of HBZ recognized by the CD4 T cells from the patient to a sequence within peptide 12: HBZ aa 111–130 (Fig. 1).

Determination of the minimum epitope sequence of HBZ recognized by CD4 T cells

Seven synthetic peptides (12-1, 12-2, 12-3, 12-4, 12-5, 12-6, 12-7) representing parts of peptide 12 were prepared (Fig. 3A). Responses of the CD4 T cells, which had been stimulated by peptide 12, to these different peptides were tested. The expanded CD4 T cells responded better to peptides 12, 12-1, 12-2, 12-3, and 12-4

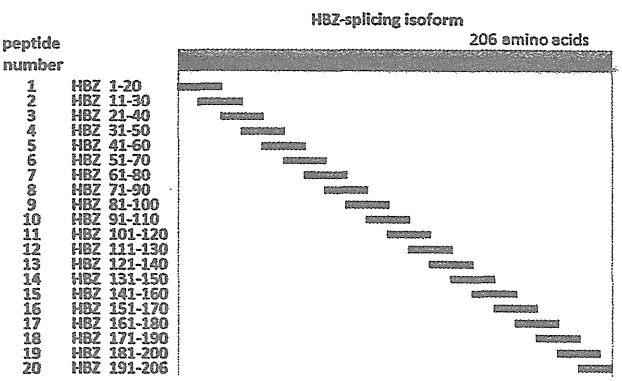

FIGURE 1. Synthetic peptides derived from spliced HBZ. Schematic of 19 20-mer and 1 16-mer synthetic peptides overlapping by 10 aa and covering the entire sequence of the spliced HBZ protein.

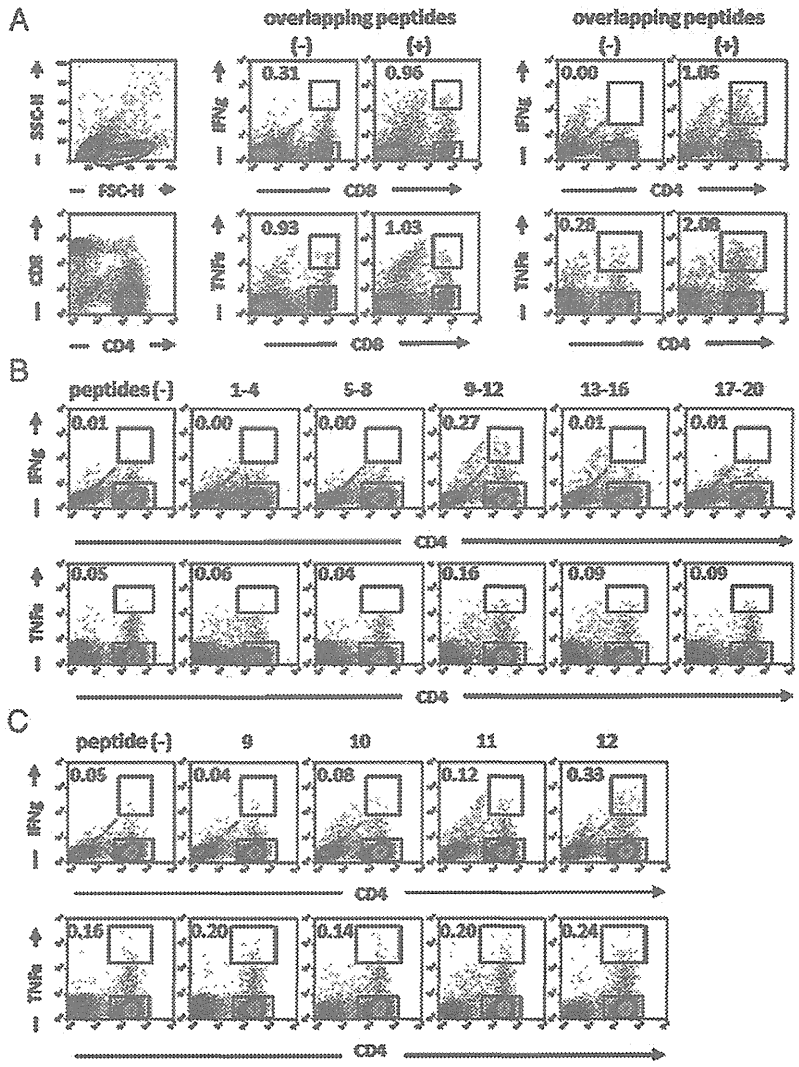

FIGURE 2. T cell responses against synthetic peptides overlapping by 10 aa and covering the entire sequence of the spliced HBZ protein. (**A**) PBMCs from patient #1 after HCT were expanded by stimulating with a mixture of 19 20-mer and 1 16-mer synthetic peptides overlapping by 10 aa and covering the entire sequence of the spliced HBZ protein. The responses of expanded CD8 and CD4 T cells to each of the overlapping peptides were evaluated by the production of IFN-γ or TNF-α. The percentage of responding cells in the upper gate ($CD8^+$ or $CD4^+$ and IFN-γ^+ or TNF-α^+ cells) relative to the cells in the lower gate ($CD8^+$ or $CD4^+$ and IFN-γ^- or TNF-α^- cells) is indicated in each flow cytometry panel. (**B**) PBMCs from patient #1 after HCT were expanded by stimulating with five overlapping peptide mixtures consisting of peptides 1–4, 5–8, 9–12, 13–16, and 17–20. (**C**) PBMCs from patient #1 after HCT were expanded by stimulating with four synthetic peptides: 9, 10, 11, and 12. The responses of expanded CD4 T cells to each synthetic peptide were evaluated by the production of IFN-γ or TNF-α. The percentage of responding cells in the upper gate relative to the cells in the lower gate is indicated in each flow cytometry panel. Each result is representative of three independent experiments.

by producing both IFN-γ and TNF-α. These cells did not respond to peptides 12-5, 12-6, or 12-7 (Fig. 3B). These data indicate that the N terminus of the minimum epitope sequence of HBZ recognized by the CD4 T cells from the patient is arginine, located at HBZ114 (Fig. 3A). Because the expanded CD4 T cells responded to peptide 12-4, the C terminus of the minimum epitope sequence of HBZ must be inside of alanine, located at HBZ125.

Next, three synthetic peptides (12-4-1, 12-4-2, 12-4-3; sequences were HBZ114–124, HBZ114–123, and HBZ114–122, respectively) were prepared to determine the C terminus of the minimum epitope sequence of HBZ (Fig. 3C). The expanded CD4 T cells responded to peptides 12-1 and 12-4 (positive controls) but not to 12-4-1, 12-4-2, 12-4-3, or a negative control peptide 12-7 (Fig. 3D). These data demonstrate that the minimum epitope sequence of HBZ recognized by the CD4 T cells from the patient was RRRAEKKAADVA (HBZ114–125).

Determination of the HLA allele on which the identified HBZ-derived peptides are presented to CD4 T cells

We investigated whether HBZ-specific CD4 T cells also recognized naturally processed and presented peptides. Thus, we initially determined *HBZ* expression by ATL or HTLV-1–immortalized cell lines and found that it was expressed by all of the lines tested (ATN-1, MT-1, MT-2, MT-4, TL-Su, TL-Om1, ATL102), regardless of their *Tax* mRNA expression (Fig. 4A, below the graph). *HBZ* expression levels of these established lines were almost as high as those of PBMCs containing >50% ATL cells obtained from 12 patients with the acute or chronic type of disease. K562 did not express *HBZ*, as might be expected, and all primary ATL cells tested were HBZ^+, consistent with an earlier study (Fig. 4A) (25). Next, we assessed the expression of HLA class II by the cell lines. The ATL or HTLV-1–immortalized cell lines tested were all positive for both HLA-DR and HLA-DQ (Fig. 4B). These observations indicate that ATN-1, MT-1, MT-2, MT-4, TL-Su, TL-Om1, and ATL102 had the potential to present the HBZ-derived peptides on their HLA-DR or HLA-DQ molecules.

Next, we examined the responses of HBZ-specific CD4 T cells from patient #1 after HCT against K562 or HBZ-expressing lines of different HLA types. The responses of HBZ-specific CD4 T cells to the lines were evaluated without the addition of peptide. The CD4 T cells that had been expanded from patient #1 after HCT using peptide 12 responded to peptide 12-1 (positive control) but not to K562, which expressed no *HBZ* (negative control) (Fig. 4C, *upper six panels*). When tested against ATL or HTLV-1–immortalized cell lines, the CD4 T cells responded strongly to ATN-1 and TL-Su (Fig. 4C, *lower panels*). Comparing the HLA class II types of the donor of the effector CD4 T cells (patient #1 after HCT) with ATN-1 and TL-Su showed that HLA-DRB1*15:01 and

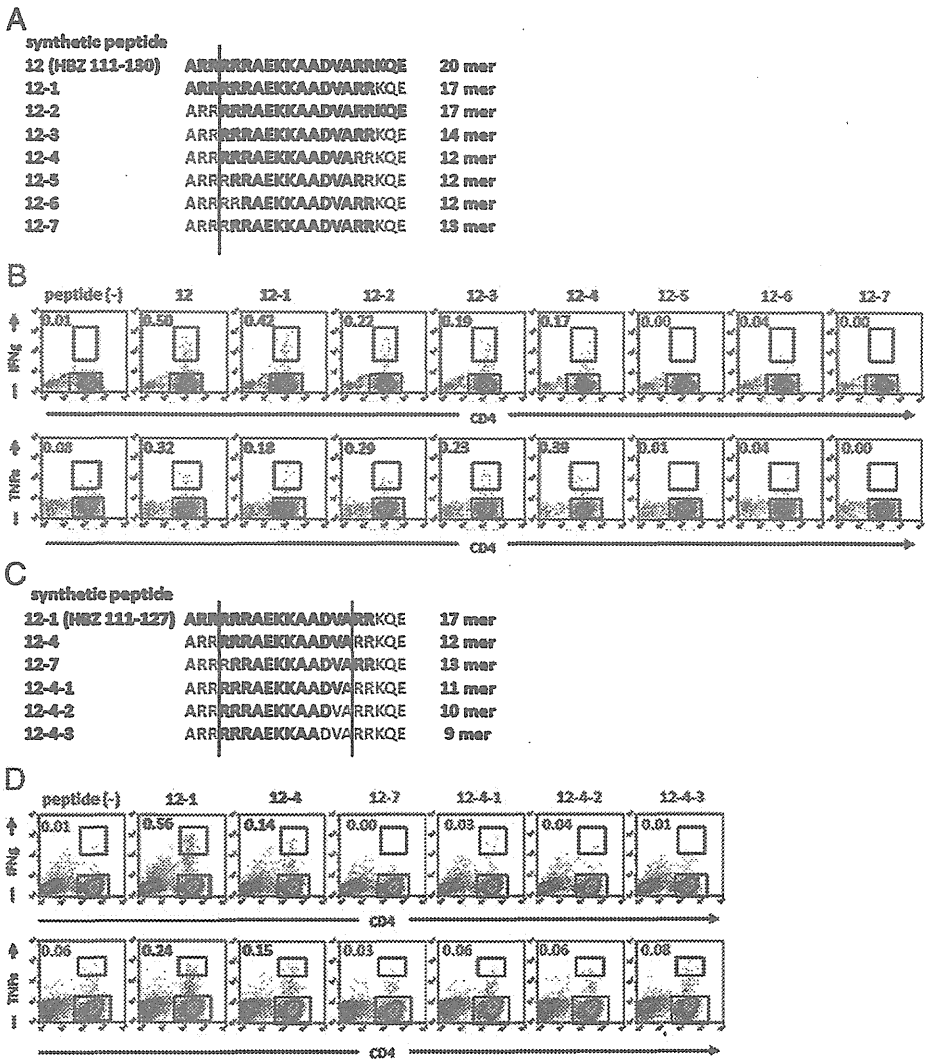

FIGURE 3. Determination of the minimum epitope sequence of HBZ recognized by CD4 T cells. (**A**) Schematic diagram of seven synthetic peptides (12-1, 12-2, 12-3, 12-4, 12-5, 12-6, 12-7) from peptide 12. They were prepared to determine the N terminus of the sequence representing the minimum epitope of HBZ recognized by the CD4 T cells. (**B**) PBMCs from patient #1 after HCT were expanded by peptide 12. The responses of expanded CD4 T cells to each synthetic peptide (12, 12-1, 12-2, 12-3, 12-4, 12-5, 12-6, 12-7) were evaluated by the production of IFN-γ or TNF-α. The percentage of responding cells in the upper gate relative to the cells in the lower gate is indicated in each flow cytometry panel. Each result is representative of three independent experiments. (**C**) Schematic diagram of three synthetic peptides (12-4-1, 12-4-2, 12-4-3) prepared to determine the C terminus of the sequence representing the minimum epitope of HBZ recognized by the CD4 T cells. (**D**) The responses of expanded CD4 T cells to each synthetic peptide (12-1, 12-4, 12-7, 12-4-1, 12-4-2, 12-4-3) were evaluated by the production of IFN-γ or TNF-α. The percentage of responding cells in the upper gate relative to the cells in the lower gate is indicated in each flow cytometry panel. Each result is representative of three independent experiments.

HLA-DQB1*06:02 were shared by all three (Table I). In addition, the CD4 T cells responded to MT-2, TL-Om1, and ATL102 to a lesser degree (Fig. 4C, *lower panels*); these three lines were found to share HLA-DRB1*15:02 and HLA-DQB1*06:01 (Table I). Together, these results indicate that the HBZ-specific CD4 T cell responses from patient #1 after HCT were restricted by HLA-DRB1*15:01 or HLA-DQB1*06:02, as well as by HLA-DRB1*15:02 or HLA-DQB1*06:01. In contrast, the peptide-sensitized CD4 T cells did not respond to MT-1 or MT-4 (Fig. 4C, *lower panels*), consistent with the present observations that the epitope of HBZ recognized by such CD4 T cells was restricted by HLA-DRB1*15:01/HLA-DQB1*06:02 and HLA-DRB1*15:02/HLA-DQB1*06:01.

Next, we tested whether HLA-DR or HLA-DQ restricted the presentation of the HBZ-derived peptide. CD4 T cells expanded by peptide 12 no longer responded to specific stimulation by peptide 12 in the presence of anti–HLA-DR–blocking mAb by producing IFN-γ (Fig. 5A, *upper left panels*), but it did respond in the presence of the isotype-control mAb (Fig. 5A, *upper right panels*). These CD4 T cells also still responded to peptide 12 in the presence of anti–HLA-DQ–blocking mAb (Fig. 5A, *lower left panels*) and its isotype control (Fig. 5A, *lower right panels*). In addition, in the presence of anti–HLA-DR–blocking mAb, CD4 T cells expanded by peptide 12 no longer responded to ATN-1 (Fig. 5B, *left panels*), which carried HLA-DRB1*15:01/HLA-DQB1*06:02 (Table I) and expressed *HBZ* mRNA (Fig. 4A). However, they did respond by producing IFN-γ and TNF-α in the presence of the isotype control (Fig. 5B, *left panels*). These CD4 T cells also still responded to ATN-1 in the presence of anti–HLA-DQ–blocking mAb and its isotype control (Fig. 5B, *right panels*). Furthermore, HBZ-specific CD4 T cell responses to K562 (negative control) were not affected by anti–HLA-DR, anti–HLA-DQ, or their isotype mAbs (Fig. 5C). These observations from Ab-blocking experiments, together with the results shown in Fig. 4, indicate that the epitope sequence of HBZ recognized by the CD4 T cells from patient #1 after HCT were restricted by HLA-DR, specifically HLA-DRB1*15:01 and HLA-DRB1*15:02.

Clinical significance of the specific CD4 T cell response against HBZ

The data presented thus far pertained to CD4 T cells obtained from only one patient (patient #1 after HCT). Therefore, we used HBZ peptide 12 to stimulate and expand 28 PBMC samples obtained from 27 other HTLV-1–infected individuals who carried HLA-DRB1*15:01 or HLA-DRB1*15:02. PBMCs were obtained from 10 HTLV-1 ACs, 10 ATL patients who had not undergone allogeneic HCT, and 8 ATL patients after allogeneic HCT. Among them, PBMCs from one individual (patient #2) were tested at different disease stages (i.e., CRs before and after allogeneic HCT). HBZ-specific CD4 T cell responses were absent in all 10

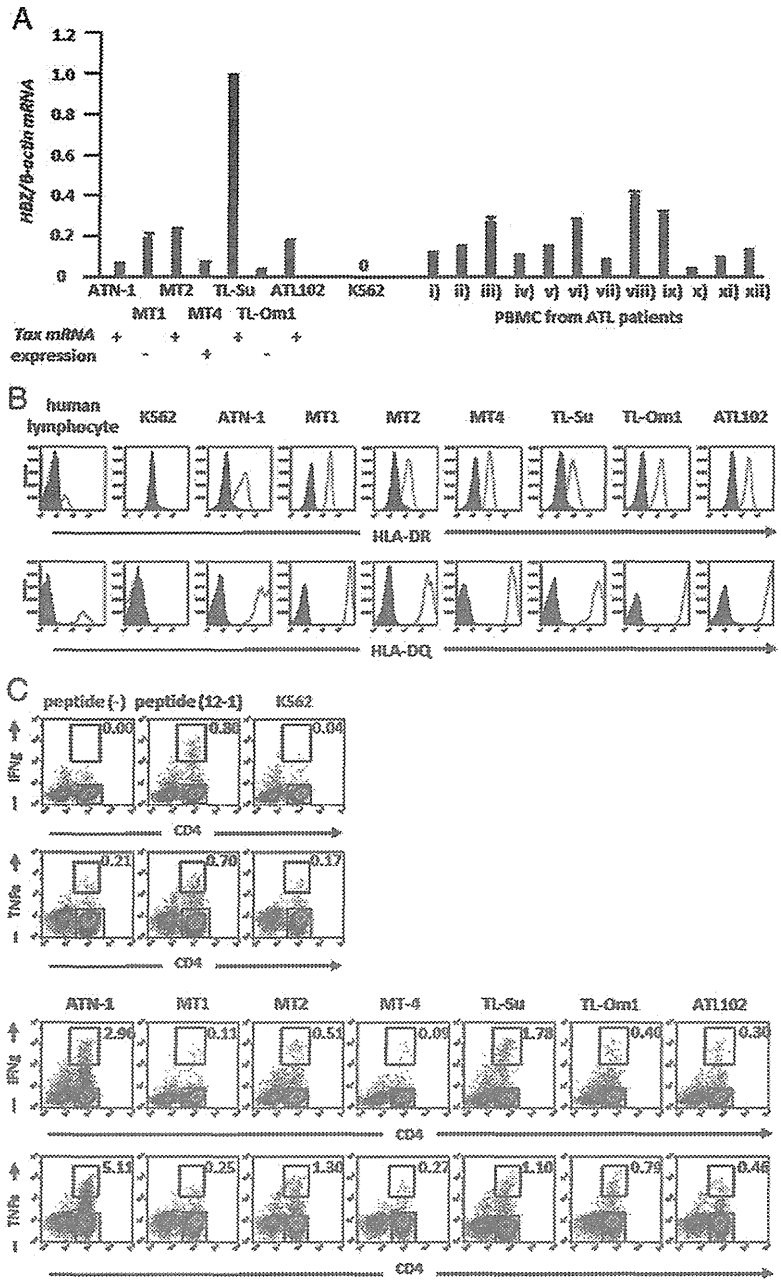

FIGURE 4. Responses of HBZ-specific CD4 T cells from patient #1 after HCT to ATL or HTLV-1–immortalized cell lines. (**A**) *HBZ* expression in ATL and HTLV-1–immortalized cell lines, K562, or PBMCs from ATL patients was analyzed by qRT-PCR by dividing the *HBZ* expression level by the *β-actin* expression level, resulting in an *HBZ/β-actin* mRNA ratio with the expression level in TL-Su set at unity. Data shown are means of triplicate experiments; error bars represent SD. *Tax* mRNA expression of each ATL and HTLV-1–immortalized cell line is indicated, as determined in our previous study (8). (**B**) HLA-DR and HLA-DQ expression in ATL cell lines, HTLV-1–immortalized lines, or K562, as analyzed by flow cytometry. The cell lines were stained with anti–HLA-DR mAb (*upper panels*, open graphs), anti–HLA-DQ mAb (*lower panels*, open graphs), or the corresponding isotype-control mAbs (filled graphs). (**C**) The expanded CD4 T cells were cocultured or not with the synthetic peptide 12-1. Negative controls without peptide stimulation (*upper left panels*) and positive controls with peptide stimulation (*upper middle panels*) are shown. The expanded CD4 T cells were cocultured with target cell lines in the absence of peptide stimulation. CD4 T cells did not respond to K562, which expressed no HBZ and acted as the negative control (*upper right panels*). The CD4 T cell responses to ATL or HTLV-1–immortalized cell lines, which expressed *HBZ*, with different HLA types were evaluated (*lower panels*). The percentage of responding cells in the upper gate relative to the cells in the lower gate is indicated in each flow cytometry panel. Each result is representative of three independent experiments.

HTLV-1 ACs, as well as in all 10 nontransplanted ATL patients (of whom 9 were in CR after systemic chemotherapy and the other was of smoldering type under observation only). In contrast, specific CD4 T cell responses to HBZ were observed in three of the eight additional ATL patients who were in CR after allogeneic HCT (patients #2, #3, and #4). The CD4 T cells from patient #2 and #4 after HCT responded to HBZ peptide 12 by producing both IFN-γ and TNF-α (Fig. 6, *right panels*). In patient #3, no TNF-α response was observed, but there was a clear IFN-γ response to HBZ peptide 12 (Fig. 6, *lower left panels*). Thus, specific CD4 T cell responses against HBZ were observed in four of nine recipients after allogeneic HCT (44%) but in no other ATL patients. Among the patients examined in this study, one patient with acute-type ATL received systemic chemotherapy and achieved CR. Subsequently, she received allogeneic HCT from an HLA-A, B, DR-matched HTLV-1 noninfected sibling donor and maintained CR (patient #2 after HCT). Although HBZ-specific CD4 T cell responses were not present at CR before allogeneic HCT in this patient (Fig. 6, *upper left panels*), they developed after transplantation (Fig. 6, *upper right panels*).

Table I. HLA information

	HLA-DRB1		HLA-DQB1		HLA-DPB1	
ATN-1	*04:05	*15:01	*04:01	*06:02	*05:01	*05:01
MT-1	*04:01	*09:01	*03:01	*03:03	*04:02	*05:01
MT-2	*04:04	*15:02	*03:02	*06:01	*05:01	*09:01
MT-4	*01:01	*16:02	*05:01	*05:02	*05:01	*05:01
TL-Su	*09:01	*15:01	*03:03	*06:02	*02:01	*17:01
TL-Om1	*15:02	*15:02	*06:01	*06:01	*09:01	*09:01
ATL102	*04:04	*15:02	*03:02	*06:01	*05:01	*09:01
Patient #1 after HCT	*04:05	*15:01	*04:01	*06:02	*02:01	*06:01

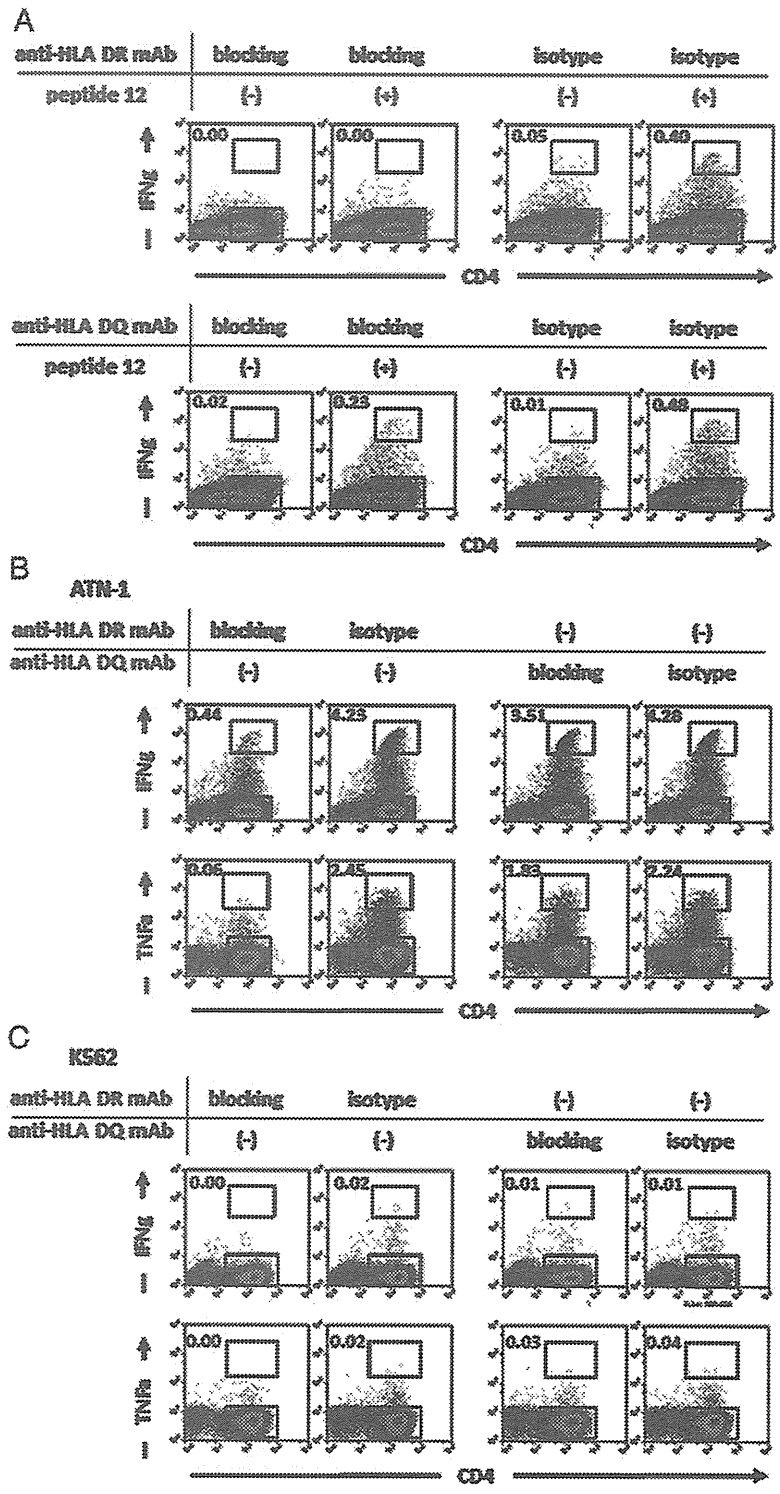

FIGURE 5. Determination of the HLA alleles restricting the presentation of HBZ-derived peptides to HBZ-specific CD4 T cells. (**A**) Responses of HBZ-specific CD4 T cells were evaluated, with or without HBZ peptide 12, in the presence of anti–HLA-DR–blocking mAb (*upper left panels*), anti–HLA-DQ–blocking mAb (*lower left panels*), or the corresponding isotype-control mAb (anti-HLA-DR isotype mAb, *upper right panels*; anti-HLA-DQ isotype mAb, *lower right panels*). Responses of HBZ-specific CD4 T cells to ATN-1, which carries HLA-DRB1*15:01/HLA-DQB1*06:02 and expresses *HBZ* mRNA (**B**), and to K562 (negative control) (**C**) were also evaluated in the presence of HLA-blocking mAbs or their isotype controls, without peptide stimulation. The percentage of responding cells in the upper gate relative to the cells in the lower gate is indicated in each flow cytometry panel. Each result is representative of three independent experiments.

Discussion

In the current study, we demonstrated the presence of HBZ-specific CD4 T cells in an ATL patient after allogeneic HCT and determined the minimum sequence of a novel HLA-DRB1*15:01–restricted HBZ-derived epitope to be RRRAEKKAADVA (HBZ114–125). HBZ peptides including the sequence HBZ114–125 were also presented on HLA-DRB1*15:02 and recognized by CD4 T cells. To the best of our knowledge, this is the first report to identify naturally processed and presented HLA-DR–restricted epitopes derived from HBZ on the surface of ATL cells. In an earlier study, an HBZ peptide–specific CTL line was established from an HLA-A*02:01^{+} individual, using peptides derived from the HBZ sequence. The peptides were selected by computer algorithms available at the BioInformatics and Molecular Analysis Section Web site (http://www-bimas.cit.nih.gov/molbio/hla_bind/) and the SYFPEITHI Web site (http://www.syfpeithi.de/) for strong binding affinity to the HLA-A*02:01 molecule. However, the established CTL line recognized the corresponding peptide-pulsed

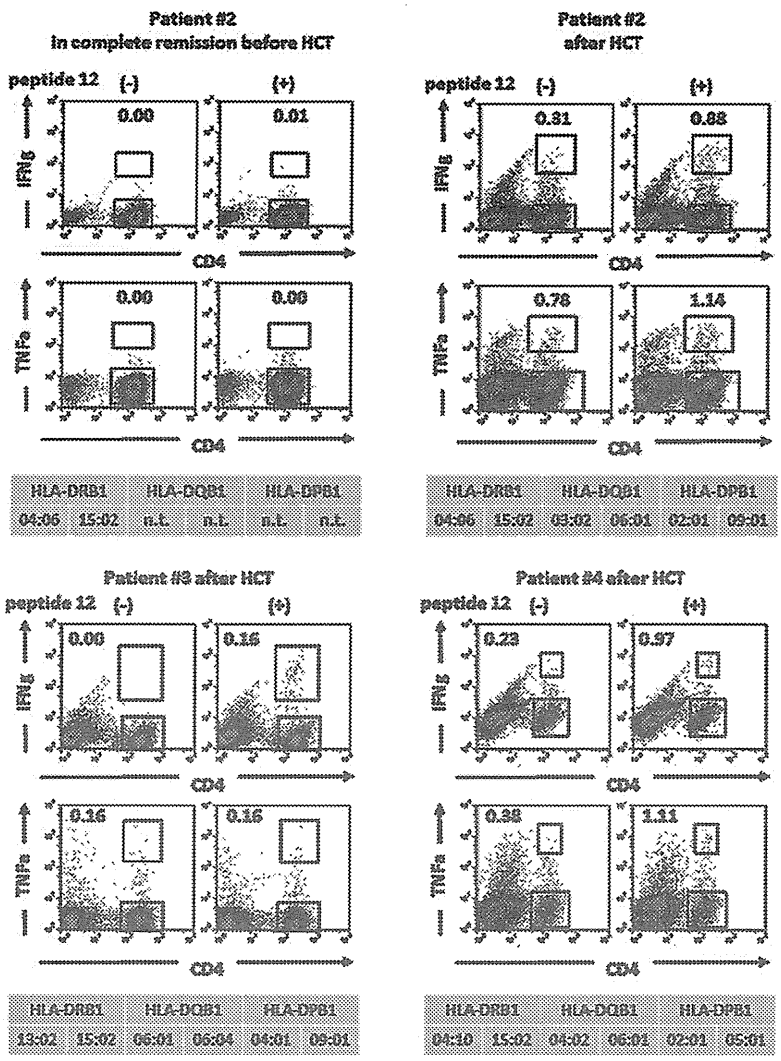

FIGURE 6. HBZ-specific CD4 T cell responses in additional ATL patients. PBMCs from additional ATL patients (#2, #3, and #4) carrying HLA-DRB1*15:02 were expanded by stimulation with HBZ peptide 12. The responses of expanded CD4 T cells to peptide 12 were evaluated by the production of IFN-γ or TNF-α. Although no HBZ-specific CD4 T cell response was observed in patient #2 in CR before allogeneic HCT (*upper left panels*), they developed after transplantation (*upper right panels*). HBZ-specific CD4 T cell responses were also observed in patient #3 (*lower left panels*) and patient #4 (*lower right panels*) in CR after allogeneic HCT. The percentage of responding cells in the upper gate relative to the cells in the lower gate is indicated in each flow cytometry panel. The HLA type of each patient is indicated below the flow cytometry panels. Each result is representative of three independent experiments. n.t., Not tested.

HLA-A*02:01$^+$ cells but not ATL cells (29). Therefore, it was not determined whether HBZ-derived peptides could be naturally presented on cells from HTLV-1–infected people. Another earlier study (30) demonstrated that HBZ expression was a critical determinant of viral persistence in the chronic phase of HTLV-1 infection. That novel study was performed using experimentally validated epitope-prediction software (34), but it did not determine the HBZ-derived epitope sequence or the corresponding HLA allele presenting it.

In the current study, no HLA-DRB1*15:01–restricted or HLA-DRB1*15:02–restricted HBZ-specific CD4 T cell response was observed in any ATL patients who had not undergone allogeneic HCT or in any HTLV-1 ACs. We surmise that HTLV-1 transmission from mothers to infants through breast milk in early life induces tolerance to HBZ, but not to Tax, by unknown mechanisms, resulting in insufficient HBZ-specific T cell responses in HTLV-1–infected individuals. This would be consistent with the persistent expression of HBZ in HTLV-1–infected cells (2, 25). In addition, insufficient HBZ-specific T cell responses may be due, in part, to the fact that the majority of the *HBZ* mRNA is retained in the nucleus, which may inhibit its translation (35), and probably leads to a low level of HBZ protein expression in HTLV-1–infected cells (29). In contrast, the finding that HLA-DRB1*15:01–restricted or HLA-DRB1*15:02–restricted HBZ-specific CD4 T cell responses were detected in ATL patients after allogeneic HCT requires explanation. Our hypothesis is that, after allogeneic HCT, the reconstituted immune system from donor-derived hematopoietic stem cells can recognize virus protein HBZ as foreign, although its expression is low, and HBZ-specific immune responses are provoked because of the lack of tolerance induction under these circumstances. In one patient with acute-type disease, HBZ-specific CD4 T cell responses were not observed in PBMCs at the time of CR before HCT, but they became detectable after allogeneic HCT. This observation supports our hypothesis. An earlier study (36) reported that HBZ-specific T cell responses were detected in some patients with HTLV-1–associated myelopathy (HAM). Unlike ATL, HAM can occur in individuals infected with HTLV-1 by any route of transmission, such as sexual intercourse (37). Therefore, some patients with HAM, infected with HTLV-1 after reaching adulthood (i.e., who became infected after their immune system had fully matured), may recognize virus protein HBZ as foreign, and HBZ-specific immune responses may be provoked. From this point of view, detection of HBZ-specific T cell responses might be expected in some HTLV-1 ACs, infected after becoming adults, but we did not see this in the present study.

In conclusion, we report the presence of HBZ-specific CD4 T cell responses in ATL patients who were in CR but only after allogeneic HCT. These responses potentially contribute to the

graft-versus-HTLV-1 effect. Novel strategies that enhance the posttransplantation allogeneic anti–HTLV-1 effect targeting HBZ, which never provokes graft-versus-host disease, could lead to improved outcomes of allogeneic HCT for ATL.

Acknowledgments

We thank Chiori Fukuyama for excellent technical assistance and Naomi Ochiai for excellent secretarial assistance.

Disclosures

T.I. received honoraria from Kyowa Hakko Kirin. The other authors have no financial conflicts of interest.

References

1. Uchiyama, T., J. Yodoi, K. Sagawa, K. Takatsuki, and H. Uchino. 1977. Adult T-cell leukemia: clinical and hematologic features of 16 cases. *Blood* 50: 481–492.
2. Matsuoka, M., and K. T. Jeang. 2007. Human T-cell leukaemia virus type 1 (HTLV-1) infectivity and cellular transformation. *Nat. Rev. Cancer* 7: 270–280.
3. Ishida, T., and R. Ueda. 2011. Antibody therapy for Adult T-cell leukemia-lymphoma. *Int. J. Hematol.* 94: 443–452.
4. Tsukasaki, K., T. Maeda, K. Arimura, J. Taguchi, T. Fukushima, Y. Miyazaki, Y. Moriuchi, K. Kuriyama, Y. Yamada, and M. Tomonaga. 1999. Poor outcome of autologous stem cell transplantation for adult T cell leukemia/lymphoma: a case report and review of the literature. *Bone Marrow Transplant.* 23: 87–89.
5. Utsunomiya, A., Y. Miyazaki, Y. Takatsuka, S. Hanada, K. Uozumi, S. Yashiki, M. Tara, F. Kawano, Y. Saburi, H. Kikuchi, et al. 2001. Improved outcome of adult T cell leukemia/lymphoma with allogeneic hematopoietic stem cell transplantation. *Bone Marrow Transplant.* 27: 15–20.
6. Ishida, T., M. Hishizawa, K. Kato, R. Tanosaki, T. Fukuda, S. Taniguchi, T. Eto, Y. Takatsuka, Y. Miyazaki, Y. Moriuchi, et al. 2012. Allogeneic hematopoietic stem cell transplantation for adult T-cell leukemia-lymphoma with special emphasis on preconditioning regimen: a nationwide retrospective study. *Blood* 120: 1734–1741.
7. Akimoto, M., T. Kozako, T. Sawada, K. Matsushita, A. Ozaki, H. Hamada, H. Kawada, M. Yoshimitsu, M. Tokunaga, K. Haraguchi, et al. 2007. Anti-HTLV-1 tax antibody and tax-specific cytotoxic T lymphocyte are associated with a reduction in HTLV-1 proviral load in asymptomatic carriers. *J. Med. Virol.* 79: 977–986.
8. Suzuki, S., A. Masaki, T. Ishida, A. Ito, F. Mori, F. Sato, T. Narita, M. Ri, S. Kusumoto, H. Komatsu, et al. 2012. Tax is a potential molecular target for immunotherapy of adult T-cell leukemia/lymphoma. *Cancer Sci.* 103: 1764–1773.
9. Masaki, A., T. Ishida, S. Suzuki, A. Ito, F. Mori, F. Sato, T. Narita, T. Yamada, M. Ri, S. Kusumoto, et al. 2013. Autologous Tax-specific CTL therapy in a primary adult T cell leukemia/lymphoma cell-bearing NOD/Shi-scid, IL-2Rγnull mouse model. *J. Immunol.* 191: 135–144.
10. Harashima, N., K. Kurihara, A. Utsunomiya, R. Tanosaki, S. Hanabuchi, M. Masuda, T. Ohashi, F. Fukui, A. Hasegawa, T. Masuda, et al. 2004. Graft-versus-Tax response in adult T-cell leukemia patients after hematopoietic stem cell transplantation. *Cancer Res.* 64: 391–399.
11. Tamai, Y., A. Hasegawa, A. Takamori, A. Sasada, R. Tanosaki, I. Choi, A. Utsunomiya, Y. Maeda, Y. Yamano, T. Eto, et al. 2013. Potential contribution of a novel Tax epitope-specific CD4+ T cells to graft-versus-Tax effect in adult T cell leukemia patients after allogeneic hematopoietic stem cell transplantation. *J. Immunol.* 190: 4382–4392.
12. Nishikawa, H., Y. Maeda, T. Ishida, S. Gnjatic, E. Sato, F. Mori, D. Sugiyama, A. Ito, Y. Fukumori, A. Utsunomiya, et al. 2012. Cancer/testis antigens are novel targets of immunotherapy for adult T-cell leukemia/lymphoma. *Blood* 119: 3097–3104.
13. Itonaga, H., H. Tsushima, J. Taguchi, T. Fukushima, H. Taniguchi, S. Sato, K. Ando, Y. Sawayama, E. Matsuo, R. Yamasaki, et al. 2013. Treatment of relapsed adult T-cell leukemia/lymphoma after allogeneic hematopoietic stem cell transplantation: the Nagasaki Transplant Group experience. *Blood* 121: 219–225.
14. Ishida, T., M. Hishizawa, K. Kato, R. Tanosaki, T. Fukuda, Y. Takatsuka, T. Eto, Y. Miyazaki, M. Hidaka, N. Uike, et al. 2013. Impact of Graft-versus-Host Disease on Allogeneic Hematopoietic Cell Transplantation for Adult T Cell Leukemia-Lymphoma Focusing on Preconditioning Regimens: Nationwide Retrospective Study. *Biol. Blood Marrow Transplant.* 19: 1731–1739.
15. Poiesz, B. J., F. W. Ruscetti, A. F. Gazdar, P. A. Bunn, J. D. Minna, and R. C. Gallo. 1980. Detection and isolation of type C retrovirus particles from fresh and cultured lymphocytes of a patient with cutaneous T-cell lymphoma. *Proc. Natl. Acad. Sci. USA* 77: 7415–7419.
16. Hinuma, Y., K. Nagata, M. Hanaoka, M. Nakai, T. Matsumoto, K. I. Kinoshita, S. Shirakawa, and I. Miyoshi. 1981. Adult T-cell leukemia: antigen in an ATL cell line and detection of antibodies to the antigen in human sera. *Proc. Natl. Acad. Sci. USA* 78: 6476–6480.
17. Gonçalves, D. U., F. A. Proietti, J. G. Ribas, M. G. Araújo, S. R. Pinheiro, A. C. Guedes, and A. B. Carneiro-Proietti. 2010. Epidemiology, treatment, and prevention of human T-cell leukemia virus type 1-associated diseases. *Clin. Microbiol. Rev.* 23: 577–589.
18. Grassmann, R., C. Dengler, I. Müller-Fleckenstein, B. Fleckenstein, K. McGuire, M. C. Dokhelar, J. G. Sodroski, and W. A. Haseltine. 1989. Transformation to continuous growth of primary human T lymphocytes by human T-cell leukemia virus type I X-region genes transduced by a Herpesvirus saimiri vector. *Proc. Natl. Acad. Sci. USA* 86: 3351–3355.
19. Tanaka, A., C. Takahashi, S. Yamaoka, T. Nosaka, M. Maki, and M. Hatanaka. 1990. Oncogenic transformation by the tax gene of human T-cell leukemia virus type I in vitro. *Proc. Natl. Acad. Sci. USA* 87: 1071–1075.
20. Akagi, T., and K. Shimotohno. 1993. Proliferative response of Tax1-transduced primary human T cells to anti-CD3 antibody stimulation by an interleukin-2-independent pathway. *J. Virol.* 67: 1211–1217.
21. Hinrichs, S. H., M. Nerenberg, R. K. Reynolds, G. Khoury, and G. Jay. 1987. A transgenic mouse model for human neurofibromatosis. *Science* 237: 1340–1343.
22. Nerenberg, M., S. H. Hinrichs, R. K. Reynolds, G. Khoury, and G. Jay. 1987. The tat gene of human T-lymphotropic virus type 1 induces mesenchymal tumors in transgenic mice. *Science* 237: 1324–1329.
23. Hasegawa, H., H. Sawa, M. J. Lewis, Y. Orba, N. Sheehy, Y. Yamamoto, T. Ichinohe, Y. Tsunetsugu-Yokota, H. Katano, H. Takahashi, et al. 2006. Thymus-derived leukemia-lymphoma in mice transgenic for the Tax gene of human T-lymphotropic virus type I. *Nat. Med.* 12: 466–472.
24. Ohsugi, T., T. Kumasaka, S. Okada, and T. Urano. 2007. The Tax protein of HTLV-1 promotes oncogenesis in not only immature T cells but also mature T cells. *Nat. Med.* 13: 527–528.
25. Satou, Y., J. Yasunaga, M. Yoshida, and M. Matsuoka. 2006. HTLV-I basic leucine zipper factor gene mRNA supports proliferation of adult T cell leukemia cells. *Proc. Natl. Acad. Sci. USA* 103: 720–725.
26. Satou, Y., J. Yasunaga, T. Zhao, M. Yoshida, P. Miyazato, K. Takai, K. Shimizu, K. Ohshima, P. L. Green, N. Ohkura, et al. 2011. HTLV-1 bZIP factor induces T-cell lymphoma and systemic inflammation in vivo. *PLoS Pathog.* 7: e1001274.
27. Fan, J., G. Ma, K. Nosaka, J. Tanabe, Y. Satou, A. Koito, S. Wain-Hobson, J. P. Vartanian, and M. Matsuoka. 2010. APOBEC3G generates nonsense mutations in human T-cell leukemia virus type 1 proviral genomes in vivo. *J. Virol.* 84: 7278–7287.
28. Takeda, S., M. Maeda, S. Morikawa, Y. Taniguchi, J. Yasunaga, K. Nosaka, Y. Tanaka, and M. Matsuoka. 2004. Genetic and epigenetic inactivation of tax gene in adult T-cell leukemia cells. *Int. J. Cancer* 109: 559–567.
29. Suemori, K., H. Fujiwara, T. Ochi, T. Ogawa, M. Matsuoka, T. Matsumoto, J. M. Mesnard, and M. Yasukawa. 2009. HBZ is an immunogenic protein, but not a target antigen for human T-cell leukemia virus type 1-specific cytotoxic T lymphocytes. *J. Gen. Virol.* 90: 1806–1811.
30. Macnamara, A., A. Rowan, S. Hilburn, U. Kadolsky, H. Fujiwara, K. Suemori, M. Yasukawa, G. Taylor, C. R. Bangham, and B. Asquith. 2010. HLA class I binding of HBZ determines outcome in HTLV-1 infection. *PLoS Pathog.* 6: e1001117.
31. Enose-Akahata, Y., A. Abrams, R. Massoud, I. Bialuk, K. R. Johnson, P. L. Green, E. M. Maloney, and S. Jacobson. 2013. Humoral immune response to HTLV-1 basic leucine zipper factor (HBZ) in HTLV-1-infected individuals. *Retrovirology* 10: 19.
32. Shimoyama, M. 1991. Diagnostic criteria and classification of clinical subtypes of adult T-cell leukaemia-lymphoma. A report from the Lymphoma Study Group (1984-87). *Br. J. Haematol.* 79: 428–437.
33. Ishida, T., A. Utsunomiya, S. Iida, H. Inagaki, Y. Takatsuka, S. Kusumoto, G. Takeuchi, S. Shimizu, M. Ito, H. Komatsu, et al. 2003. Clinical significance of CCR4 expression in adult T-cell leukemia/lymphoma: its close association with skin involvement and unfavorable outcome. *Clin. Cancer Res.* 9: 3625–3634.
34. MacNamara, A., U. Kadolsky, C. R. Bangham, and B. Asquith. 2009. T-cell epitope prediction: rescaling can mask biological variation between MHC molecules. *PLOS Comput. Biol.* 5: e1000327.
35. Rende, F., I. Cavallari, A. Corradin, M. Silic-Benussi, F. Toulza, G. M. Toffolo, Y. Tanaka, S. Jacobson, G. P. Taylor, D. M. D'Agostino, et al. 2011. Kinetics and intracellular compartmentalization of HTLV-1 gene expression: nuclear retention of HBZ mRNAs. *Blood* 117: 4855–4859.
36. Hilburn, S., A. Rowan, M. A. Demontis, A. MacNamara, B. Asquith, C. R. Bangham, and G. P. Taylor. 2011. In vivo expression of human T-lymphotropic virus type 1 basic leucine-zipper protein generates specific CD8+ and CD4+ T-lymphocyte responses that correlate with clinical outcome. *J. Infect. Dis.* 203: 529–536.
37. Yamano, Y., and T. Sato. 2012. Clinical pathophysiology of human T-lymphotropic virus-type 1-associated myelopathy/tropical spastic paraparesis. *Front. Microbiol.* 3: 389.

Kinpara et al. Retrovirology 2013, 10:52
http://www.retrovirology.com/content/10/1/52

RETROVIROLOGY

RESEARCH Open Access

Interferon-α (IFN-α) suppresses HTLV-1 gene expression and cell cycling, while IFN-α combined with zidovudin induces p53 signaling and apoptosis in HTLV-1-infected cells

Shuichi Kinpara[1,2], Mami Kijiyama[1], Ayako Takamori[1], Atsuhiko Hasegawa[1], Amane Sasada[1], Takao Masuda[1], Yuetsu Tanaka[3], Atae Utsunomiya[4] and Mari Kannagi[1*]

Abstract

Background: Human T-cell leukemia virus type-1 (HTLV-1) is the causative retrovirus of adult T-cell leukemia/lymphoma (ATL) and HTLV-1-associated myelopathy/tropical spastic paraparesis (HAM/TSP). HTLV-1 gene expression is maintained at low levels *in vivo* by unknown mechanisms. A combination therapy of interferon-α (IFN-α) and zidovudin (AZT) shows therapeutic effects in ATL patients, although its mechanism is also obscure. We previously found that viral gene expression in IL-2-dependent HTLV-1-infected T-cells (ILTs) derived from ATL patients was markedly suppressed by stromal cells through a type I IFN response. Here, we investigated the effects of IFN-α with or without AZT on viral gene expression and cell growth in ILTs.

Results: ILTs expressed variable but lower amounts of HTLV-1 Tax protein than HTLV-1-transformed HUT102 cells. Following the addition of IFN-α, the amounts of HTLV-1 p19 in the supernatants of these cells decreased in three days, while HTLV-1 gene expression decreased only in ILTs but not HUT102 cells. IFN-α also suppressed the spontaneous HTLV-1 induction in primary ATL cells cultured for 24 h. A time course study using ILTs revealed that the levels of intracellular Tax proteins decreased in the first 24 h after addition of IFN-α, before the reduction in HTLV-1 mRNA levels. The initial decreases of Tax protein following IFN-α treatment were observed in 6 of 7 ILT lines tested, although the reduction rates varied among ILT lines. An RNA-dependent protein kinase (PKR)-inhibitor reversed IFN-mediated suppression of Tax in ILTs. IFN-α also induced cell cycle arrest at the G0/G1 phase and suppressed NF-κB activities in these cells. AZT alone did not affect HTLV-1 gene expression, cell viability or NF-κB activities. AZT combined with IFN-α markedly induced cell apoptosis associated with phosphorylation of p53 and induction of p53-responsive genes in ILTs.

Conclusions: IFN-α suppressed HTLV-1 gene expression at least through a PKR-mediated mechanism, and also induced cell cycle arrest in ILTs. In combination with AZT, IFN-α further induced p53 signaling and cell apoptosis in these cells. These findings suggest that HTLV-1-infected cells at an IL-2-dependent stage retain susceptibility to type I IFN-mediated regulation of viral expression, and partly explain how AZT/IFN-α produces therapeutic effects in ATL.

Keywords: ATL, HTLV-1, IFN-α, PKR, Innate immunity, Anti-viral therapy, AZT, p53

* Correspondence: kann.impt@tmd.ac.jp
[1]Department of Immunotherapeutics, Graduate School of Medical and Dental Sciences, Tokyo Medical and Dental University, 1-5-45 Yushima, Bunkyo-ku, Tokyo 113-8519, Japan
Full list of author information is available at the end of the article

Background

Human T-cell leukemia virus type 1 (HTLV-1) causes adult T-cell leukemia/lymphoma (ATL) [1-3], a malignant lympho-proliferative disorder resistant to chemotherapy. The virus is also responsible for HTLV-1-associated myelopathy/tropical spastic paraparesis (HAM/TSP) [4,5], a chronic inflammatory demyelinating disorder. Despite such severe clinical outcomes, levels of HTLV-1 gene expression are thought to be very low *in vivo*. HTLV-1 mRNA, but not proteins, are detectable in peripheral blood mononuclear cells (PBMCs) of HTLV-1-infected individuals [6]. Although undetectable, a low level of HTLV-1 proteins must be present *in vivo*, as HTLV-1-infected individuals maintain antibodies against HTLV-1 structural proteins and Tax protein-specific cytotoxic T lymphocytes.

Recent therapeutic approaches, such as allogeneic hematopoietic stem cell transplantation (allo-HSCT) [7,8], a humanized antibody therapy targeting CCR4 [9,10], or anti-viral therapy with interferon (IFN)-α and zidovudin (AZT) [11-13] partly improved ATL prognosis. *Ex vivo* studies have indicated that graft-versus-tumor responses including anti-Tax cytotoxic T-cells were potentially involved in the therapeutic mechanisms of allo-HSCT [14], and that the CCR4-antibodies were capable of inducing antibody-dependent cellular cytotoxicities [15]. However, combining AZT/IFN-α hardly affects HTLV-1-infected cells *in vitro* [16], and the mechanisms of its therapeutic effects remain unclear. A recent report indicated that the triple combination of arsenic trioxide/IFN-α/AZT demonstrated more favorable therapeutic effects in ATL patients [17]. The combination of arsenic trioxide and IFN-α has been reported to induce proteolysis of Tax in HTLV-1-infected cells *in vitro* [18,19]. As IFN-α is indispensable in AZT/IFN-α, arsenic trioxide/IFN-α or arsenic trioxide/IFN-α/AZT therapies, ATL cells might be susceptible to IFNs *in vivo*.

It is well established that HTLV-1-infected cells are resistant to type I IFNs *in vitro*. For example, IFN-α reduced the virus release but not viral protein synthesis in HTLV-1-transformed HUT102 or MT-2 cells [20]. The mechanisms of the resistance to type I IFNs in HTLV-1-infected cells include reduction in the phosphorylation of Tyk2 and STAT2 [21], Tax-mediated competition with CREB binding protein/p300 [22], Tax-mediated up-regulation of SOCS1 [23,24], and up-regulation of IRF4 [25], all of which result in inhibition of IFN signaling. This may explain why IFN-α combined with AZT does not affect HTLV-1-infected cells *in vitro*, while conflicting with the clinical effects of AZT/IFN-α therapy in ATL patients. This discrepancy between *in vivo* and *in vitro* systems can be partially attributed to differences in status of HTLV-1-infected cells between the two systems.

We previously found that HTLV-1-infected cells could induce type I IFN responses in co-cultured stromal cells [26]. We also found that viral expression in HTLV-1-infected T-cells is markedly suppressed at both mRNA and protein levels through type I IFN responses mediated by stromal cells co-cultured [26]. This observation again conflicts with the previous notion of HTLV-1-mediated resistance to type I IFNs *in vitro*. Our experimental system differed from previous studies in two ways. First, we used IL-2-dependent HTLV-1-infected T-cells (ILTs) derived from ATL patients, while previous studies used IL-2-independent HTLV-1-transformed cell lines such as HUT102. Second, we used stromal cells as effectors; these mediated the type I IFN response, but could have also produced multiple factors other than IFNs.

In the present study, we investigated whether purified type I-IFNs can affect viral expression and cell growth of HTLV-1-infected cells by using various ILTs. Here we report a novel finding that IFN-α suppresses intracellular Tax expression at a translational level at least through PKR. We further demonstrate that IFN-α activates p53 pathways in cooperation with AZT, partly explaining the mechanisms of the therapeutic effects of AZT/IFN-α in ATL.

Results

Effects of IFN-α on HTLV-1 p19 release and viral transcription

We evaluated the baseline levels of HTLV-1 gene expression in HUT102, ILT-Hod and ILT-#29 cell lines (Figure 1A). Relative levels of HTLV-1 mRNA in ILT-Hod and ILT-#29 cells were comparable with those in HUT102 cells. However, the levels of Tax protein in ILT-Hod and ILT-#29 cells were much lower than those of HUT102, and were barely detectable by immunoblotting only after stimulation of ILTs with phorbol 12-myristate 13-acetate (PMA). Flow cytometry results also indicated that ILT-Hod and ILT-#29 cells expressed smaller amounts of intracellular Tax protein than HUT102 cells. In addition, our analyses often identified Tax-negative cell populations in ILTs, with the ratio of these populations fluctuating during culture. These cells are also HTLV-1-infected, as all the cells in ILT-Hod and ILT-#29 cultures express HTLV-1 Gag protein after stimulation with PMA (Figure 1A insert), suggesting a dynamic turnover of HTLV-1 proteins in ILTs. Tax expression in HUT102 cells was apparently stable (Figure 1A).

We added IFN-α at various concentrations (300, 3000, and 30000 IU/ml) on HUT102, ILT-Hod, and ILT-#29 cells (Figure 1B). The amounts of HTLV-1 p19 released in supernatants significantly decreased after 72 h in culture for all the cell lines tested. Gag mRNA levels were also decreased in ILT-Hod and ILT-#29 in 3 days of culture (Figure 1B). These suppressive effects were observed at all doses of IFN-α used, indicating that 300 IU/ml of IFN-α was sufficient to produce these effects.

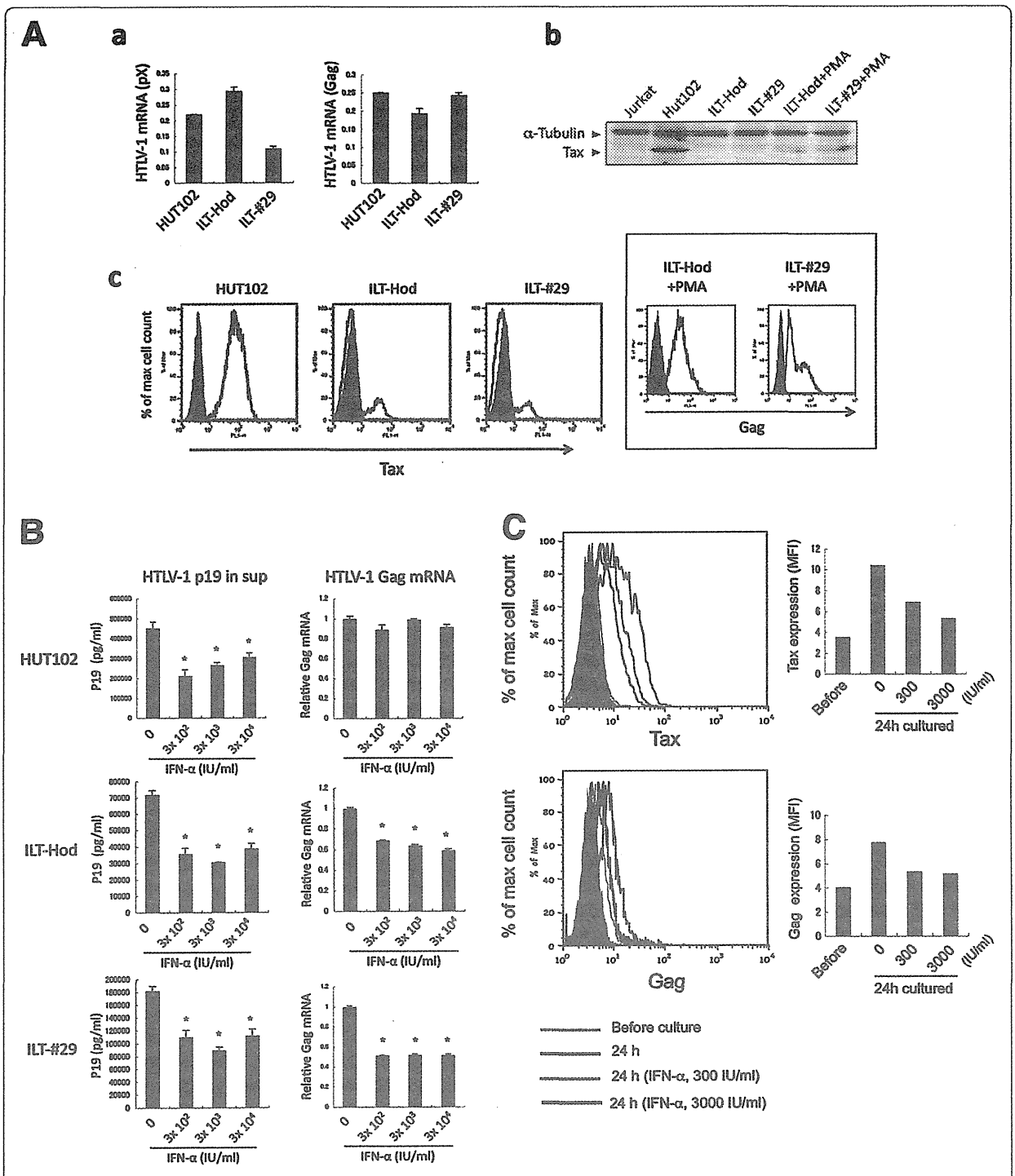

Figure 1 (See legend on next page.)